1977

Tests and analysis of beam-to-column web connection, June 1977

G. P. Rentschler

W. F. Chen

G. C. Driscoll Jr.

Beam-to-Column Connections

TESTS AND ANALYSIS OF BEAM-TO-COLUMN WEB CONNECTION DETAILS

By

Glenn P. Rentschler
and
Wai-Fah Chen

This work has been carried out as part of an investigation sponsored jointly by the American Iron and Steel Institute and the Welding Research Council.

Department of Civil Engineering
Fritz Engineering Laboratory
Lehigh University
Bethlehem, Pennsylvania

May 1977

Fritz Engineering Laboratory Report No. 405.7

LEHIGH UNIVERSITY
BETHLEHEM, PENNSYLVANIA 18015
TELEPHONE (215) 691-7000

DEPARTMENT OF CIVIL ENGINEERING
FRITZ ENGINEERING LABORATORY #13
405

July 11, 1977

MEMORANDUM

TO: Members, WRC Task Group on Beam-to-Column Connections

J. A. Gilligan	N. W. Edwards	H. A. Krentz
V. V. Bertero	W. E. Edwards	W. A. Milek, Jr.
O. W. Blodgett	H. J. Engstrom, Jr.	C. W. Pinkham
V. R. Cartelli	E. R. Estes, Jr.	A. N. Sherbourne
H. C. Crick	T. R. Higgins	F. W. Stockwell, Jr.
C. F. Diefenderfer	I. M. Hooper	N. Young

FROM: G. C. Driscoll

SUBJECT: (1) Fritz Engineering Laboratory Report No. 405.7
(2) July 20 Task Group Meeting

Enclosed you will find Fritz Engineering Laboratory Report No. 405.7 entitled "Tests and Analysis of Beam-to-Column Web Connection Details". This report describes the results of the completed web connection pilot test program. Please bring this report with you to the meeting.

Also enclosed is a tentative agenda for the meeting. At the end of the agenda you will see which reports you should bring with you to the meeting. The meeting will be held in Room 117, Sinclair Laboratory, on the Lehigh Campus. This is the same location as last year's meeting. Please note that the starting time has been changed to 9:00 A.M. Based on the returns of your attendance slips, there will be a good representation of Task Group members (13 yes, 3 no).

We look forward to seeing you at the meeting.

G. C. Driscoll

Enclosure
cc: H. Bandel
R. Bjorhovde
W. F. Chen
C. R. Felmley, Jr.
W. C. Hansell
A. C. Kuentz
H. S. Lew
F. Schneller
I. M. Viest
Project Staff

TABLE OF CONTENTS

1. INTRODUCTION

1.1 Background

One of the most influential elements in the behavior and cost of multistory steel building frames is the moment resisting beam-to-column connection. A majority of these connections are column flange connections where the beam frames into the column flange. Considerable research work has been done on this type of connection at Lehigh University (1,2,3) as well as many other research institutions [(5,6), for example].

However, another type of moment resisting connection commonly found in building frames is the column web connection. In this connection, the beam is attached to the column perpendicular to the plane of the column web (Fig. 1). The action of the beam bending moment tends to bend the column about its weak axis. It is a study of this type of connection which is currently underway at Lehigh University.

The previous research done on column web connections in the United States was limited to static loading tests of symmetric web connections (4) and tests of unsymmetrical web connections under repeated and reversed loading (5) with no axial force. The current research work at Lehigh University centers on a study of unsymmetrical web connections where there is only a beam on one side of the column (Fig. 1) and where there is axial load applied on the column. This is a more severe type of loading on the beam and column assemblage than the symmetrically loaded connections previously studied. This study is under the guidance of the Welding Research Council Task Group on Beam-to-Column Connections.

1.2 Scope

The study of beam-to-column web connections is divided into two distinct phases of activity. Each phase consists of both experimental and theoretical investigations.

The first phase of activity is called the pilot test program. In attempting to organize a comprehensive research program of web connections, it was felt that, by isolating certain variables, a better insight into different aspects of connection behavior could be obtained. Since the study centers around moment-resisting web connections, the critical variable chosen to be examined prior to the development of full-scale connection assemblages was the effects that concentrated forces resulting from beam bending have on a column when applied in a way to simulate a web connection. For this pilot study, the effects of column axial load and beam shear on the behavior of the web connections were ignored. The main purpose of the pilot tests was to gain knowledge for use in the design of full-scale specimens. The results of the pilot test program are presented here. A report presenting the details of the pilot test program, including description of the specimens, is given in Ref. 7.

The second phase is the testing of four full-scale web connections. Each assemblage will consist of an 18-ft. long column and a beam approximately 5 ft. long connected at mid-height of the column. Four different geometries of welding and bolting the beam to the column will be tested. These connections will simulate actual building connections with the beam transmitting shear and moment to the column and the column carrying axial load. The details of this phase of activity including a

description of the specimens and test setup are given in Ref. 8. Results of the full-scale testing program will be presented in a later report.

2. PILOT TEST DESCRIPTION

2.1 Objective

For the beam-to-column web connection assemblage shown in Fig. 1, the theoretical maximum strength of this assemblage is reached when plastic hinges are formed at sections X and Y in the column or in the beam. For the case of hinges in the column without axial load, this would occur when a moment of M_p is reached at X and Y (M_{pc} for a column with axial load).

However, there exist other factors that limit this maximum strength. For example, when the beam flange is narrower than the distance between column fillets and the beam is welded directly to the column web (Fig. 2, Test A), a yield line mechanism may form in the column web before the formation of plastic hinges at X and Y in the column. This depends on the width of beam flange, depth of beam and column web thickness. When the attachment of the beam to the column is such that the yield line mechanism will not form, the maximum load based on simple plastic theory might not be attained due to local buckling of the column flanges and web. Further, the assemblage could be prevented from reaching its maximum strength by fracture or punching shear failure of the plate material.

If the loading of the beam is required to reach a magnitude that exceeds the values of a yield line mechanism or a local buckling load, the concept of stiffening the column must be considered.

Thus, the overall objective of these pilot tests can be viewed as a study of the behavior and strength based on simple plastic theory,

yield line theory, local buckling, fracture and the related needs of stiffening, should the maximum strength of the connection be required to carry the beam load.

More specifically, the objectives of the moment pilot tests are:

1. A study of the behavior and ultimate strength of the column web under the action of concentrated flange forces representing the beam end moment.
2. A study of the different methods of attaching the beam flanges to the column in web connections.
3. A study of the stiffener requirements on the side of the column opposite the beam.

These results were sought to be used as the basis for the development of tests of full-scale web connection assemblages.

2.2 Test Program

The pilot test program was composed of eight different test specimens. Two different column sizes were utilized, one from a typical upper story and one from a typical lower story of a multistory building. The two column shapes and the plates attached to them, hereafter referred to as plates, flange plates, or flange connection plates, which were utilized to simulate the concentrated beam moment forces were made of ASTM A572 Grade 50 steel. This is the same steel that was planned for the full-scale tests. With each column size, four geometries of attaching the simulated beam flange plates to the column were tested. The two column sections used were a W14x184 and a W12x106. The four different connection geometries are shown in Fig. 2 and labelled as Tests A through D. It should be pointed out that the specimens were proportioned so

that the plastic hinge formed in the column prior to yielding of the moment plates.

Tests A and B represent the cases where the beam flange is narrow enough to fit between the flanges of the column (actually between the fillets of the column). As was stated previously, the theoretical maximum strength of the web connection assemblage is the formation of plastic hinges in the column. For light beam loading cases, a maximum strength based on the formation of a yield line mechanism may be sufficient.

The design of Test A was to achieve a yield line mechanism (Fig. 3) and observe its behavior, pattern and associated strength. The tests sought experimental evidence to check the existing yield line solutions (9,10). Further, this test would provide an opportunity to assess stiffening requirements necessary to prevent formation of the yield line mechanism when the strength of the column hinge mechanism is required. Even if the yield line mechanism strength is sufficient, column stiffening may still be required because of the interaction of local column web deformations and the axial load.

As the beam flange width increases, a point is reached at which the yield line mechanism can not form. Test B in Fig. 2 was such a case; the beam flange was so wide (fillet to fillet) that a yield line mechanism could not form. It was the intent with this test to observe whether the column plastic hinge mechanism can be attained or whether local buckling of the column flanges could intervene under column axial load prior to reaching this load. If local buckling is a possibility,

stiffening criteria must be developed. Fracture of material at the fillets is also very critical in this case.

Tests C and D simulated the case of beam flange connection plates having a width equal to the distance between column flanges. These tests would represent, among others, the case where a beam flange is wider than the distance between column flanges, thus necessitating a narrowing flange connection plate or the case of a bolted flange connection, again necessitating a flange connection plate.

Tests C and D were similar to Test B. However, if Test B was controlled by fracture, Tests C and D should attain the column mechanism load without premature fracture. If local buckling of the column flange is a possibility under axial load, stiffening criteria again must be developed to enable these connections to reach their maximum strength. The effects of different welding geometries on the strength of web connections could also be examined in Tests C and D.

2.3 Test Setup

The test setup is shown in Figs. 4 and 5. The column shape was placed horizontally on two supports and loaded at two points by means of a spreader beam. With this setup, one test could be conducted on each end of the column. Because of the centrally placed machine load, a load of P/2 would go into each tension plate. Figure 4, Sec. A-A shows the method of transferring the load of P/2 around the column section using a yoke so that it could be applied as a concentrated tensile load to one of the plates. The compression reaction and the applied tensile load at each end of the column provided the force couple needed to simulate the beam moment. In these tests, no axial force was applied to the column.

When one test on a setup reached its useful limit, the yoke for that particular test could be supported, preventing deflection in order that the other test might be completed. For each of the two column sections, Tests A and B were tested simultaneously, as were Tests C and D.

2.4 Specimen Description

The eight pilot tests were designated as 12A through 12D and 14A through 14D. The 12 indicates that the test (A through D) was performed on the W12x106 shape and the 14 refers to the W14x184 shape. For the specimens tested on the W12x106 column shape, the distance between tension and compression plates was 14 in. For the W14x184 column, the distance between the two plates was 24 in. Shown in Table 1 is a chart giving a summary of the distinguishing features of the pilot test specimens.

A view of Specimens 12A and B and 14A and B is shown in Fig. 6. For all four of these tests, the plates were welded to the column by full penetration groove welds. Tests 12A was composed of 1"x7" plate. Test 14A was designed with a 1¼"x6¼" plate. Tests 12B and 14B were designed with a plate width equal to the distance between column k-lines. For Specimen 12B, this required a 1"x9½" plate and for Specimen 14B, a 1"x11¼" plate. The plate thicknesses for all specimens were designed so that the tests could be completed without yielding of the plates.

Specimens 12C and D and 14C and D are shown in Fig. 7. Tests 12C and 14C were fillet welded with the plate welded on both sides to the column web and flanges. For 12C, the plate was 1"x10-15/16" with a 3/8 in. fillet weld and for 14C, the plate was 1"x12-5/8" with a 3/8 in. fillet weld.

Tests 12D and 14D were fillet welded with the plate welded on both sides to the column flanges only. For 12D, the plate was a 1½"x 10-15/16" with an 11/16 in. fillet weld, and for 14D, the plate was 1½"x12-5/8" with an 11/16 in. fillet weld. The plates for Test D were thicker than those of Test C because a larger thickness was required to prevent shear yielding of the plates adjacent to the flange fillet welds. The gap between the end of the plates and the column web was 3/4 in. for the W12x106 and 1 in. for the W14x184.

3. RESULTS OF PILOT TESTS

A total of eight pilot tests have been conducted. The results of each of these tests will now be discussed in detail. Table 2 gives a summary of test results for all eight pilot tests.

3.1 Test 12A

A photograph showing the failure of Specimen 12A is presented in Fig. 8. Failure of this specimen was caused by fracture of the column web material in the region of the tension plate. No such fracture occurred in the region of the compression plate. The test failed at a testing machine load of 292 kips (146 kips tension and compression plate load). The extent of column web yielding in the panel zone between the tension and compression plate is shown in Fig. 9. From the figure, it is evident that yielding progressed through the entire region but the pattern only slightly resembles the yield line pattern in Fig. 3. This will be more fully discussed in Sec. 4. Much of the yielding was concentrated near the two plates with the region near the tension plate, at right in the figure, showing more yielding than the compression plate region. For this test, the plate width of 7" was 74% of the distance between column k-lines.

Shown in Fig. 10 is a plot of the overall deflection of the tension plates of Tests 12A and 12B. These plots reflect the overall behavior of the connections and include items such as the bending of the column acting as a beam, column web deformation, and elastic deformation of the tension and compression plates. The dashed line in the figure is a theoretical elastic load-deflection curve assuming the column to act

as a beam loaded by two equal concentrated loads at the tension plate locations and merely accounts for bending of the column. Also shown in this figure, are the values of $P_{y\ell}$ and P_p which are, respectively, the loads required to cause the theoretical yield line mechanism (Fig. 3) of the column web of Test A and the plastic hinge mechanism of the column. As is evident from the figure, the maximum load for Test 12A was well below P_p, as could be expected, but it also was far below the yield line load $P_{y\ell}$. The maximum testing machine load on Test 12A was 292 kips which is 77 percent of $P_{y\ell}$. The testing machine load at which fracture of the column web initiated was 250 kips (125 kips flange load) and is obvious by the change in stiffness at this point in Figs. 10, 11 and 13. At this load level, there already was some yielding of the column web indicated by flaking whitewash.

Figures 11 and 13 show, respectively, plots of the column web and column flange movements. The column web deflections are deflections of the web from its original plane (measured relative to the junction of the column web and flanges). These out-of-plane deformations are significant as they can be magnified in the presence of a column axial load and may cause local buckling of these elements. Shown in Fig. 15 is a view of the flange deformations which occurred in Test 12A.

3.2 Test 12B

Test 12B was designed with a broad tension and compression flange plate width equal to the distance between column k-lines. Photographs showing this specimen at failure are given in Figs. 16 and 17. The failure of Test 12B was due to fracture of the column web material at

the ends of the tension plate. Figure 17 gives a view of the column web from the side opposite the tension plate showing clearly the fracture of the column web. No fracture was evident in the region of the compression plate. The test reached a maximum testing machine load of 334 kips. The extent of yielding of the column web in the panel zone is shown in Fig. 18. Here, the yielding is basically concentrated at the two plates with more yielding occurring in the area around the tension plate (at right in figure) than at the compression plate.

Shown in Fig. 10 is a plot of the tension plate deflection versus testing machine load for Test 12B. Since the flange plates were so wide that the theoretical yield line mechanism could not form, it was felt that this test might be able to attain P_p, the plastic hinge mechanism of the column. However, Fig. 10 shows the maximum load for Test 12B was 334 kips which is only 64 percent of P_p. The initiation of fracture of the column web in this specimen occurred at a testing machine load of 326 kips (163 kips flange load) and this is evident from Figs. 10, 12 and 14. Again on this test, there was some yielding of the column web prior to fracture. Also, in Fig. 10, the elastic stiffness of Test 12B is greater than Test 12A as would be expected due to the wider flange plates of Test 12B.

Shown in Figs. 12 and 14, are plots of the column web and column flange movements. These displacements are less than those of Test 12A in the elastic region but they are still of such significant magnitude that they may be important in the presence of a column axial force. In Fig. 14, at high loads, the column flange movement adjacent to the compression plate is influenced greatly by the column flange movement adjacent to the tension plate even though the plates are 14 inches apart.

3.3 Tests 12C and 12D

Because of their similar behavior, Tests 12C and 12D will be discussed together. The tension plate deflection of both specimens is shown in Fig. 19. As is evident from the figure, both specimens reached P_p, the plastic hinge mechanism load of the column. The maximum testing machine load for these two tests was 568 kips compared with the P_p load of 524.6 kips. Shown in Fig. 20 is a view of the column section for Tests 12C and 12D showing the yielding of the column flange, further supporting the conclusion that the specimens reached P_p. In contrast to Tests 12A and 12B, the column flange and column web deformations of Tests 12C and 12D were insignificant (web deflection and column flange movement were respectively .008 in. and .019 in. at maximum load adjacent to the tension flange plate of Test 12C). However, it should be pointed out that both these deflection quantities were larger for Test 12C than for Test 12D because of some force being transferred to the column web. Therefore, the deflection plotted in Fig. 19 is reflective of the deflection of the column section as a simply supported beam acted upon by two concentrated loads. The dotted line in the figure is a theoretical elastic-plastic load deflection curve of a W12x106 column shape acting as such a beam. Also shown, is an elastic slope line (also dotted) including the effects of shortening and lengthening of the compression and tension plates on the deflection. These two tests had to be terminated when the compression plates, which acted as supports, experienced bending, induced by the large bending deflections and related rotations of the column.

Shown in Fig. 21 is a view of the compression plate of Test 12D. Test 12D had the tension and compression plates fillet welded only to

the column flanges. Therefore, the large forces in the two plates had to be transferred from the plates to the column flanges over a short distance through shear stress. This plus residual stresses in the plates due to welding along the column flanges caused these plates to exhibit early yielding adjacent to the fillet welds as shown in Fig. 21.

3.4 Test 14A

Photographs showing the failure of Specimen 14A are shown in Figs. 22 and 23. The failure of this specimen was caused by fracture of the column web material near the ends of the tension plate as shown. No fracture of the column web material occurred at the ends of the compression plate. Figure 23 is a view of the column web from the side opposite the tension plate showing the fracture of the web material. The test reached a maximum testing machine load of 414 kips before failure. The extent of yielding in the panel zone for this specimen is shown in Fig. 24. The yielding is essentially concentrated near each of the tension and compression plates. The column web at the tension plate (at right in photograph) shows considerably more yielding than the web at the compression plate. The yielding of the column web does not reach to the midpoint of the two loading plates and, therefore, does not resemble the yield line mechanism (Fig. 3). For this test, the plate width of 6¼" was 55% of the distance between column k-lines.

Shown in Fig. 25 is a plot of the tension plate deflection of 14A and 14B. The tension plate deflection is reflective of the overall connection behavior. Shown on this graph are the values of $P_{y\ell}$ and P_p. The sloping dashed line is a theoretical elastic load-deflection curve assuming the column to act as a beam loaded by two equal concentrated

loads at the tension plate locations and merely accounts for bending of the column. As is evident from Fig. 25, Test 14A failed to achieve P_p, as might be expected, but it also failed to reach the yield line load $P_{y\ell}$. The maximum load reached was 89 percent of $P_{y\ell}$. The flange load at which fracture of the column web initiated was 175 kips (350 kips machine load) and is clearly obvious by the change in stiffness of the connection at this point in Figs. 25, 26 and 28. As in Tests 12A and 12B some yielding of the column web was observed prior to the load at which fracture occurred.

Figures 26 and 28 show the relatively large movements of the column web and flanges, respectively. In an actual case, this out-of-plane deformation shown in Figs. 26 and 28 can be accentuated by the column axial force and local buckling of the flange or web elements could occur. Shown in Fig. 30 is a photo during testing depicting the large flange movements of both specimens. Test 14A is in the foreground and Test 14B is to the rear.

Comparing Fig. 26 with Fig. 11, it is evident that the web deflection of Test 14A is much greater than 12A at the point of fracture. This is due mainly to the wider web of the 14 inch column and the narrower tension plate (relative to distance between column k-lines) of 14A producing greater web flexibility.

3.5 Test 14B

A photograph showing the failure of specimen 14B is given in Fig. 31. The failure of Test 14B was again due to the fracture of the column web material near the ends of the tension plate. The column web adjacent

to the compression plate did not fail. The test reached a maximum testing machine load of 504 kips. The extent of yielding on the column web panel zone is shown in Fig. 32. There is considerably more yielding on the column web at the tension plate (at right in figure) than at the compression plate. This specimen had tension and compression plates of a width equal to the distance between column k-lines.

Shown in Fig. 25 is the testing machine load versus the tension plate deflection for Test 14B and its comparison to the plastic hinge mechanism load P_p. The maximum test load was 87 percent of P_p. As indicated by the drastic change in slope on the load-deflection curve in Fig. 25, the fracture of Test 14B initiated at a load of 500 kips. It is also interesting to note on Fig. 25 that the elastic stiffness of Test 14B was greater than that of Test 14A as would be expected due to the wider plate of Test 14B.

Shown in Figs. 27 and 29 are plots of the column web and column flange movements, respectively, for Test 14B. These displacements are significant, although somewhat less than those of 14A. From Fig. 29 it can be seen that, although the tension and compression plates are 24 in. apart, at high loads, the movement of the column flanges at the tension plate starts to affect the column flange displacement at the compression plate.

3.6 Tests 14C and 14D

Specimens 14C and 14D will be discussed together because their behavior was similar. The tension plate deflection of both specimens is shown in Fig. 33. Both of these specimens had sufficient strength to

develop the plastic hinge mechanism load P_p as shown in the figure. The maximum testing machine load of Tests 14C and 14D was 598 kips as compared to the P_p load of 580 kips (the P_p load and $P_{y\ell}$, the yield line load for all specimens were calculated using actual steel yield strengths determined from coupon tests). Since the relative deflections of the column webs and column flanges were very small, the deflection plotted in Fig. 33 is solely reflective of the deflection of the column section as a simply supported beam acted upon by two concentrated loads. The dotted line in the figure is the theoretical elastic-plastic load deflection curve of the W14x184 column shape acting as such a beam. Also shown, is an elastic slope line including the effects on the deflection of shortening and lengthening of the compression and tension plates, respectively. The tests were terminated when the deflection of the column acting as a beam became large so that the beam rotations near the compression plates, which acted as supports, caused bending in the compression plates.

The maximum column web and flange movements were respectively .005 and .025 for Test 14C adjacent to the tension flange plate. The comparable deflections for 14D were even smaller because there was no force transferred from the tension plate to the column web.

Although both connections performed adequately, there was some yielding on the compression plate near the welds of 14D as shown in Fig. 34. This is because Test 14D had the tension and compression plates welded only to the column flanges and the large axial force had to be transferred from the plates to the column flanges over a short distance through shear stress. This, plus the residual stresses induced in the

plate due to the fillet welding along the column flanges caused these plates to exhibit early yielding adjacent to the fillet welds.

The results of Tests 14C and 14D, as well as the previously described results of Tests 12C and 12D, show that the additional welding of the flange plates to the column web may not be necessary. This conclusion is valid as long as the welds of the plates to the column flanges are sufficient and as long as the plates are thick enough to preclude extensive shear yielding adjacent to these welds.

4. THEORETICAL DISCUSSION

4.1 General

Theoretical predictions of the maximum load were based on two possible modes of failure. These were, first, a yield line mechanism similar to the one in Fig. 3, and second, formation of plastic hinges in the column. For Test A, with plates welded only to the column web and well clear of the column flange fillets, the load prediction based on a yield line mechanism was substantially lower than the load based on formation of plastic hinges in the column. For Tests B, C, and D, it was predicted that formation of plastic hinges in the column would be the limiting mechanism.

The experimental results for Tests C and D did achieve their predicted strength. These tests will, therefore, be discussed only briefly. Test B, with a wide plate nearly spanning the distance between column web fillets, can be considered as the limiting case for application of a yield line mechanism. Neither this test nor Test A reached the loads predicted for them. In the following, the yield line theory will be discussed and observations made as to why the predicted loads were not reached for Test A and Test B. Consideration will also be made of other possible failure modes which might permit more accurate predictions to be made.

4.2 Yield Line Theory (10)

For the yield line pattern shown in Fig. 3, and assuming (a) all lines in the assumed yield line pattern are stressed to F_y, the yield strength of the column material, and (b) that the web surface

enclosed by lines (1) and (2) remains plane, the expression for internal work along the yield lines is:

$$W_I = \frac{2F_y}{d}\left[\left(\frac{bd}{12} + \frac{da}{6}\right)t + \left(\frac{b}{2} + \frac{d^2}{2a}\right)t^2 + \frac{6t^3d}{a}\right]\Delta$$

where

b = flange plate width

d = distance between flanges

a = one-half of the value of the distance between column fillets minus flange width

t = thickness of column web

Δ = deflection under flange plate.

The external work is

$$W_{EXT} = 2P_{y\ell}\Delta$$

where

$P_{y\ell}$ = force in one flange required to cause the yield line mechanism.

Equating external work with internal work and solving for $P_{y\ell}$ gives

$$P_{y\ell} = \frac{F_y}{d}\left[\left(\frac{bd}{12} + \frac{da}{6}\right)t + \left(\frac{b}{2} + \frac{d^2}{2a}\right)t^2 + \frac{6t^3d}{a}\right]$$

4.3 Comparison of Yield Line Theory with Test Results for Tests A and B

On the two tests conducted where the yield line mechanism might have been expected to develop (Tests 12A and 14A), the maximum loads reached were 77 percent and 89 percent, respectively, of the theoretical yield line loads. A previous paper on the yield line mechanism has recognized the attainment of the full yield line load $P_{y\ell}$ is not always possible and suggested that the theoretical load be factored by more than

just the load factor (12). However, the most important finding is that the mode of failure was not predicted by the yield line mechanism. The yielding on the column web was concentrated around each of the tension and compression plates and did not appear to extend to midway between the two plates. The yielding of the column web around the tension plate was more severe than around the compression plate. In effect, the specimens did not behave according to assumption (b) of the yield line theory. This assumption stated that the web surface between the two flange plates remains plane.

The eventual failure of the specimens was due to fracture of the web plate at the ends of the tension flange plates. Fracture did not occur in the column web at the flange compression plates. The fracture was probably caused by triaxial tension in the column web at the two ends of the tension plate caused by the tension plate force and the out-of-plane deformations of the column web.

It is usually assumed that the stress in the tension plate is uniform over its width and thickness. However, strain gages which were placed on the tension plate indicate that the stress is higher at the edges than at the middle. This is shown qualitatively in Fig. 35. Shown in Fig. 36 is a plot of the strains measured at five locations across the width of the tension plate of Test 14A. It can be deduced from this plot that the strains (and related stresses) are much higher at the edges of the plate than in the middle. This can be explained from the viewpoint of the flexibility of the web plate. The web plate midway between the two column flanges is relatively flexible. Due to the constraint offered by the column flanges, the column web stiffness

increases significantly near the column flanges. Hence, as a force is applied to either the tension or compression plate, the higher stress in the plate will occur in the region of greater stiffness, i.e., the edge of the plate adjacent to the column flange. This higher than nominal P/A stress, along with the sharp discontinuities at the edges, is what accentuated the triaxial tension to produce fracture at the ends of the tension plate. Test data also shows that as the ratio of the plate width to clear distance between column flanges increases, the difference between the maximum stress to the minimum stress in Fig. 35 increases. This is because, as the plate becomes wider, the edges are closer to the stiff column flanges and consequently, more stress in the plate is attracted to the plate edges. The compression plate also produced a triaxial state but no fracture because one of the major stresses was compression.

Test B is one where the yield line theory would not apply because the plate was too wide to allow the yield line pattern in Fig. 3 to develop. This test was expected to develop the plastic moment of the column. However, because of the stiffness situation and the triaxial tension stress state, the Test B specimens failed by fracture in a similar manner to that of Test A specimens. The triaxial stress situation is less of a contributor here to fracture than in Test A because of the smaller out-of-plane movement of the column web in Test B.

In an actual column web moment connection, the beam web is usually attached to the column web in some way to transmit the beam shear to the column. If this took the form of a vertical plate welded to the column web nearly the full depth of the beam, the moment applied

to a connection similar to that of Test A could probably be increased beyond the load reached on the present tests. Because of this shear plate, the column web would be forced to remain plane between the tension and compression beam flanges and, hence, the web stiffness would be more uniform and the final mechanism should be closer to that of Fig. 3 rather than the nonuniform stress distribution and localized failure mode observed in Test A. However, the stress concentrations near the edge of the tension plate will not be helped by such a shear plate. This stress concentration plus additional constraint provided by welding of another plate onto the column web will not alleviate the fracture conditions of the material. Hence, it could negate any increase in load caused by the full development of the yield line mechanism.

An observation can be made with regard to the load-deflection behavior of Test 14A as seen in Figs. 25, 26 and 28. The initiation of fracture of the column web is shown by the large decrease in stiffness of the connection. At this point, the column web has deformed out-of-plane to a large extent, allowing significant membrane stress to enter the picture (shown schematically in Fig. 37). Thus, from this point on in the loading, the fracture situation tends to reduce the load carrying capacity while the membrane stress, rather than the bending stress of the column web, tends to allow an increase in load. By examining Fig. 25, it shows that the increase of the membrane stress exceeds the localized material tearing and the load continues to increase beyond the initial fracture point. This phenomenon does not occur in Test 12B or 14B because the plates are so wide and the out-of-plane deflection of the column web remains relatively small, not allowing the membrane action of the column web to show up. By examining the last two columns of

Table 2, it is apparent that there is not much increase in load of Test 12B and 14B beyond initial fracture, most probably due to the absence of any membrane effect.

The membrane effect does not appear in Test 12A for basically the same reason it does not occur in Tests 12B or 14B. For Test 12A, the flange plates are 7 inches wide or 74 percent of the distance between the column k-lines. This is a relatively wide plate when compared to the 6½ inch wide plate of Test 14A which is only 55 percent of the k-line distance. Thus, for Test 12A, the out-of-plane deformation of the column web is small compared to that of Test 14A as is evident by a comparison of Figs. 11 and 26. Therefore, for Test 12A, the fracture condition tending to reduce the load far exceeds any membrane effect, preventing much of an increase in load beyond initial fracture.

4.4 Effect of Connection Type on Column Web Stresses

As might be expected, the four different types of connections of the flange plates to the column affect the column web to different degrees. Shown in Fig. 38 is a plot of strain in the column web versus tension flange plate force for the four connections on the W12x106 shape. The strain is measured by a linear strain gage placed on the opposite side of the column web from the tension flange plate and centered midway across the web between the two column flanges. [This measurement of strain largely reflects the amount ~~at~~ of bending in the column web caused by the tension flange plate.]

The column webs for Tests 12A and 12B were the most severely stressed. This result is expected because these two types have no connection to the column flanges and therefore all the tension plate force goes directly into the web. Test 12A had higher strains than Test 12B because of the longer span of flexible column web exposed by the narrower tension flange plate of 12A.

For the other two tests, the column web of Test 12C experienced more strain than the web of 12D. This again is expected because in 12C the tension flange plate was welded to the column web in addition to being welded to the column flanges. In Test 12D, there was no weld of the tension flange plate to the column web. The small strains that do exist in the web of 12D are probably the result of some out-of-plane movement of the column flanges due to Poisson's effect in the tension flange plate.

The interesting observation which can be made here is that on Test 12C, even though there was no stiffener placed in the column on the opposite side from the tension flange plate, it appears that there was a significant amount of the tensile flange force making its way into the column web. Prior to this, it was a common belief that the web carried little or no force (similar to Test 12D) with the absence of opposite side column stiffening.

4.5 Stress Distribution in Flange Plates for Tests C and D

Shown in Fig. 39 is a qualitative plot of strain in the tension flange plates of Tests C and D details. These are plots of trends which were observed for each load level in Tests 14C and 14D measured by the three linear gages shown.

The difference in the two strain distributions lies in the ratio of the maximum strain at the plate edges to the minimum strain at the plate center. The ratio is larger for Test D than for Test C. This observation can be explained by the fact that in Test D there was no welding to the column web and all of the flange plate force must be transferred to the column by the two column flange welds. This requires the stress in the plate to concentrate more toward the plate edges than in Test C where the column web is relied upon to accept a portion of the plate force. The high stress concentrations in Test D detail must be accounted for in designing.

5. CONCLUSIONS

A series of eight pilot tests have been conducted to observe the performance of simulated beam-to-column web connections under the effects of an applied beam bending moment. These pilot tests are the first phase of a study on the behavior of a beam-to-column web connections, the next being the testing of four full-scale web connection assemblages.

The pilot test specimens were in the form of W12 and W14 columns with plates welded perpendicular to the column webs and loaded to simulate the action of beams framed into a column web. The distinguishing features of each test are given in Fig. 2 and Table 1. Two of the series simulated connections in which the beam flange plates are welded only to the column web. Of these, Test A had a relatively narrow beam flange plate and Test B had a wide beam flange plate nearly reaching the column flange fillets. The other two series simulated connections in which the beam flanges or flange connection plates are wide and are fitted between and welded to the column flanges. The Test C beam flange plate was welded to the column web as well, but in Test D it was not welded to the column web.

The following conclusions can be made regarding the test results of Phase 1--Pilot Tests:

1. The yield line mechanism of Test A (Fig. 3) is not fully developed because of early fracture of material. The actual maximum test loads were 77 and 89 percent, respectively, for Tests 12A and 14A of that predicted by the yield line theory presented in Ref. 10. The yield line mode obtained was more

localized about the flange plates than that predicted in Article 4.

2. Test B on both column shapes failed to develop the fully plastic moment of the column section due to fracture of column web caused by a nonuniform stress concentration in the tension plate.
3. The failure of Test A on both the W12x106 and W14x184 columns was fracture of the column web material due to triaxial tension caused by the column web deformation and by nonuniform stress concentrations.
4. The nonuniform stress distribution in the flange plates was instrumental in causing fracture of the column web in Tests A and B. This nonuniform stress distribution appears to be accentuated as the ratio of the flange plate width to column web depth increases.
5. Test A and Test B connections exhibited no fracture problems in the region adjacent to the flange compression plate.
6. The use of some type of connection of the beam web to the column web for Test A could possibly change the yield line mode. However, it is questionable whether such a connection would achieve the yield line mechanism load predicted in Article 4.
7. Large column web and column flange out-of-plane deformations are associated with Tests A and B. These deformations may be important when considering local buckling of a column under a high axial load.
8. The large column web deformations in type A and B connections may have an effect on steel building frame analysis and design.
9. Test B connections exhibited greater stiffness than Test A connections.

10. For flange plates with a width small in comparison to the distance between column k-lines, connections of the Test A type may increase in strength beyond initial fracture due to the membrane effect of the column web.
11. Tests C and D reached the maximum load associated with developing a plastic hinge in the column.
12. There were no significant out-of-plane deformations of the column web and column flanges on Tests C and D as there were in Tests A and B. Local buckling appears not to be a problem.
13. Even without the use of a stiffener on the opposite side of a column web from a flange plate, the column web has enough stiffness to carry some of the flange plate load in Test C.
14. Connections using Type D detail are sufficient but they must be also adequately designed to prevent possible yielding of flange adjacent to flange weld.

It is evident that in the design of beam-to-column web connections, precautions must be taken to reduce the chance of fracture as well as allowing for design limits based on forming plastic hinges in the column or forming a yield line mechanism in the column web.

6. ACKNOWLEDGMENTS

The investigation reported herein was conducted in the Fritz Engineering Laboratory of Lehigh University, Bethlehem, Pennsylvania. Dr. L. S. Beedle is Director of the Laboratory and Project Director.

The study of steel beam-to-column web connections is sponsored jointly by the American Iron and Steel Institute and the Welding Research Council. Research work is carried out under the technical guidance of the WRC Task Group on Beam-to-Column Connections, of which Mr. John A. Gilligan is Chairman. The interest, encouragement and guidance of this committee is gratefully acknowledged.

A special note of thanks is given to Mr. J. A. Gilligan and Mr. W. E. Edwards for their comments on the first draft of this manuscript and to Dr. G. C. Driscoll for his thorough review of the final version of this report.

7. REFERENCES

1. Huang, J. S., Chen, W. F. and Beedle, L. S., "Behavior of Design of Steel Beam-to-Column Moment Connections," Welding Research Council Bulletin No. 188, October 1973.

2. Parfitt, J., Jr. and Chen, W. F., "Tests of Welded Steel Beam-to-Column Moment Connections," Journal of the Structural Division, ASCE, Vol. 102, No. ST1, January 1976.

3. Standig, K. F., Rentschler, G. P. and Chen, W. F., "Tests of Bolted Beam-to-Column Flange Moment Connections," Welding Research Council Bulletin (to appear).

4. Graham, J. D., Sherbourne, A. N., Khabbaz, R. N. and Jensen, C. C., "Welded Interior Beam-to-Column Connections," American Institute of Steel Construction, 1959.

5. Popov, E. P. and Pinkney, R. B., "Cyclic Yield Reversal in Steel Building Connections," Engineering Journal, AISC, Vol. 8, No. 3, July 1971.

6. Bose, S. K., "Analysis and Design of Column Webs in Steel Beam-to-Column Connections," Ph.D. Dissertation, University of Waterloo, March 1970.

7. Rentschler, G. P. and Chen, W. F., "Program of Pilot Tests Associated with Beam-to-Column Web Connection Studies," Fritz Engineering Laboratory Report No. 333.28, Lehigh University, Bethlehem, Pa., August 1974.

8. Rentschler, G. P. and Chen, W. F., "Test Program of Moment-Resistant Steel Beam-to-Column Web Connections," Fritz Engineering Laboratory Report No. 405.4, Lehigh University, Bethlehem, Pa., May 1975.

9. Kapp, R., "Yield Line Analysis of a Web Connection in Direct Tension," Engineering Journal, AISC, Second Quarter, 1974.

10. Stockwell, F. W., Jr., "Yield Line Analysis of Column Webs with Welded Beam Connections," Engineering Journal, AISC, First Quarter, 1974.

11. Fielding, D. J. and Chen, W. F., "Steel Frame Analysis and Connection Shear Deformation," Journal of the Structural Division, ASCE, Vol. 99, No. ST1, January 1973.

12. Abolitz, A. L. and Warner, M. E., "Bending under Seated Connections," Engineering Journal, AISC, January 1965.

Table 1

Distinguishing Features of Pilot Test Specimens

Beam Flange Plate Welded to Column WEB ONLY	
NARROW Beam Flange Plate	WIDE Beam Flange Plate
Test A 12A 14A	Test B 12B 14B

Beam Flange Plate Welded Between Column FLANGES	
Welded to Column Web	NOT Welded to Column Web
Test C 12C 14C	Test D 12D 14D

Table 2

Comparison of Theoretical Maximum Flange Forces to Test

Test	Yield Line or Plastic* Hinge Mechanism (kips) (1)	Initial Load at Tearing (2)	Maximum Test Load (kips) (3)	(2)/(1)	(3)/(1)
12A	190.4	125	146	.66	.77
12B	262.3	163	167	.62	.64
14A	231.5	175	207	.76	.89
14B	290	250	252	.86	.87
12C&12D	262.3	---	284	---	1.08
14C&14D	290	---	299	---	1.03

*Yield line for Tests 12A and 14A; plastic hinge mechanism for other tests.

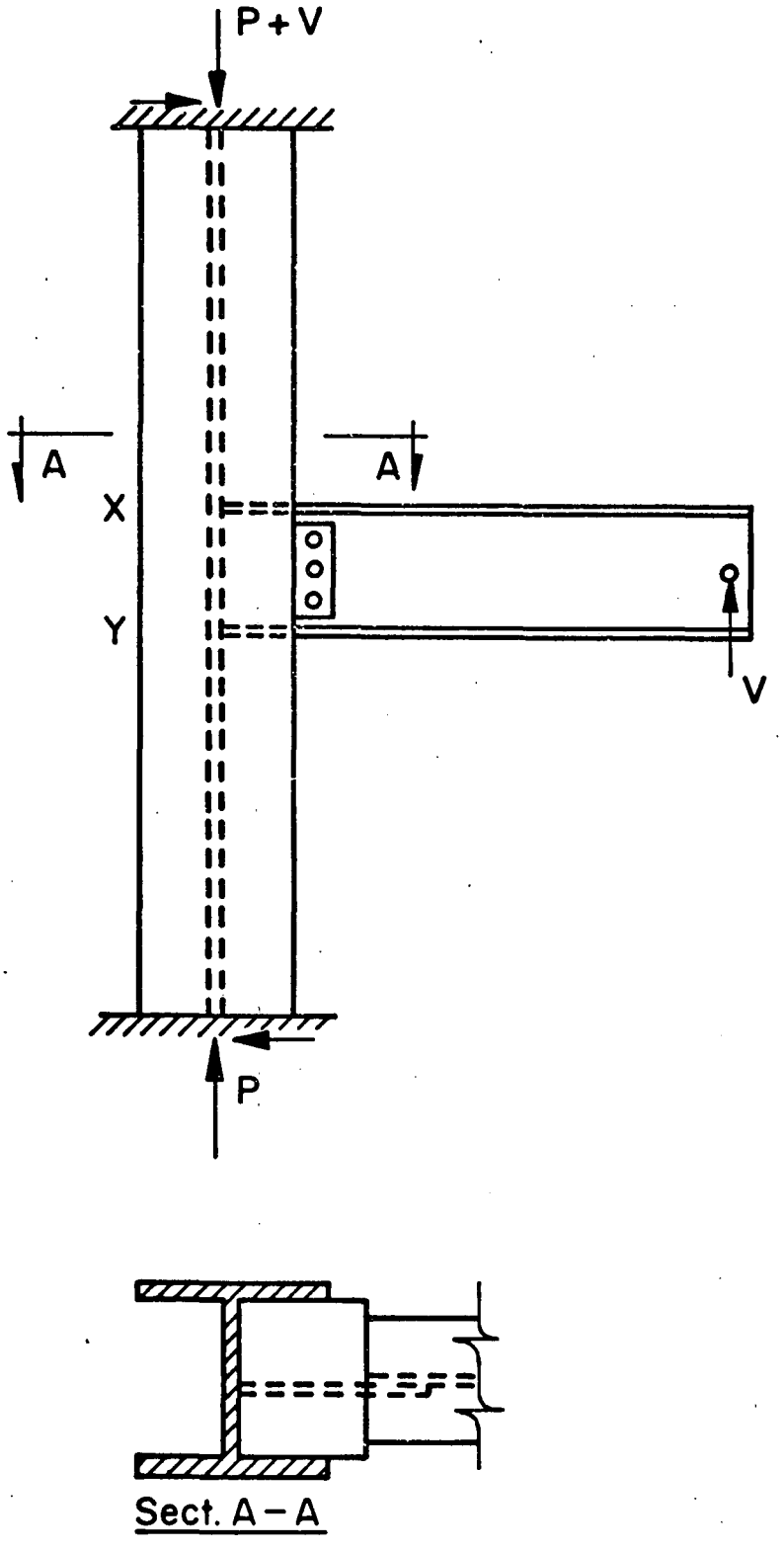

Fig. 1 Web Connection Assemblage

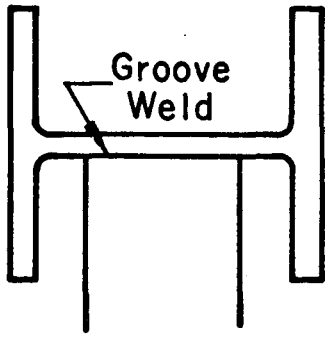

Test A

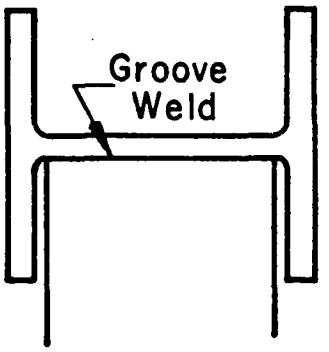

Test B

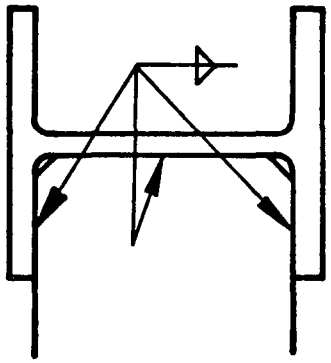

Test C

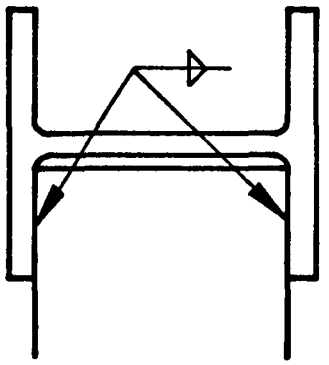

Test D

Fig. 2 Pilot Test Connection Schemes

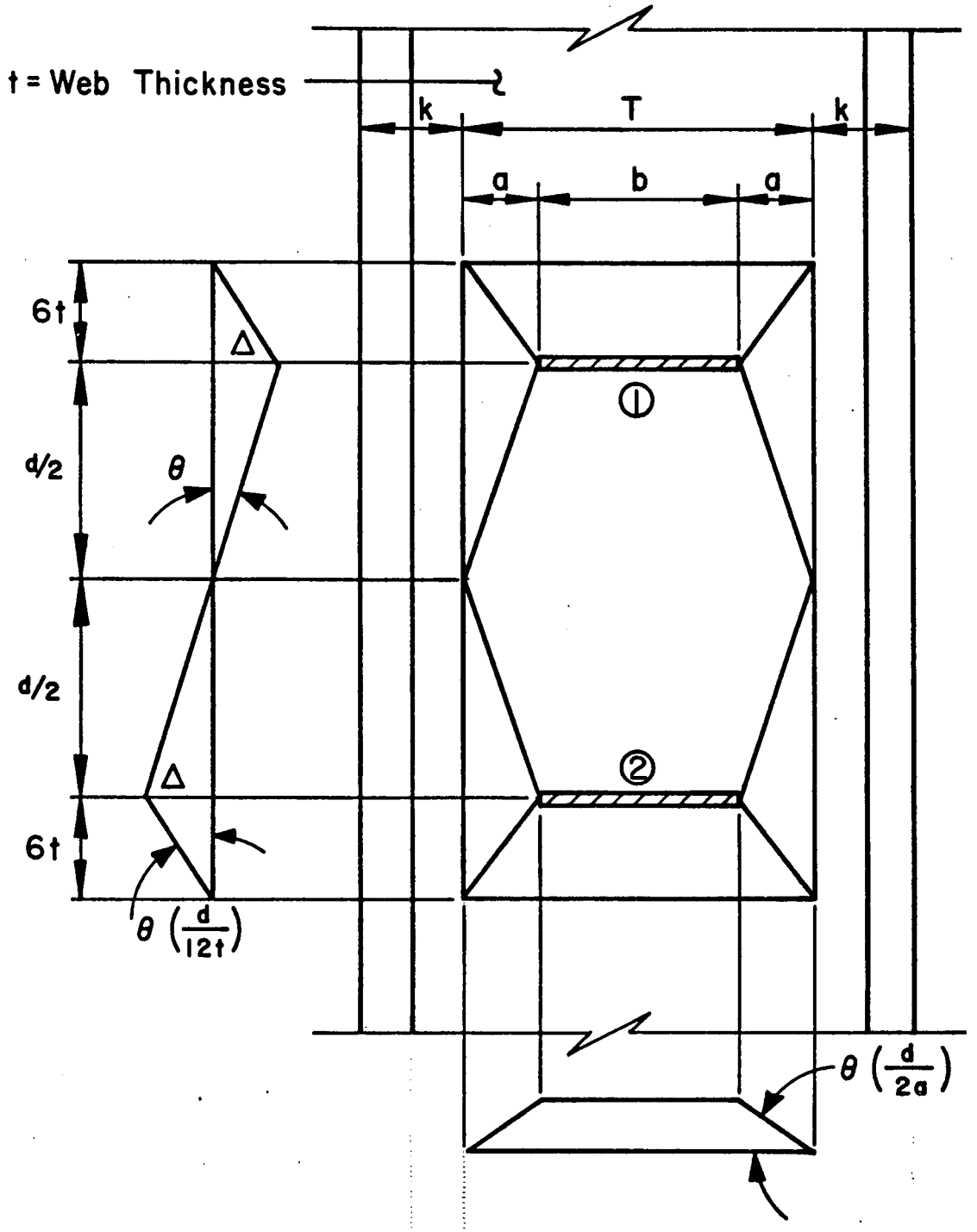

Fig. 3 Column Web Yield Line Pattern

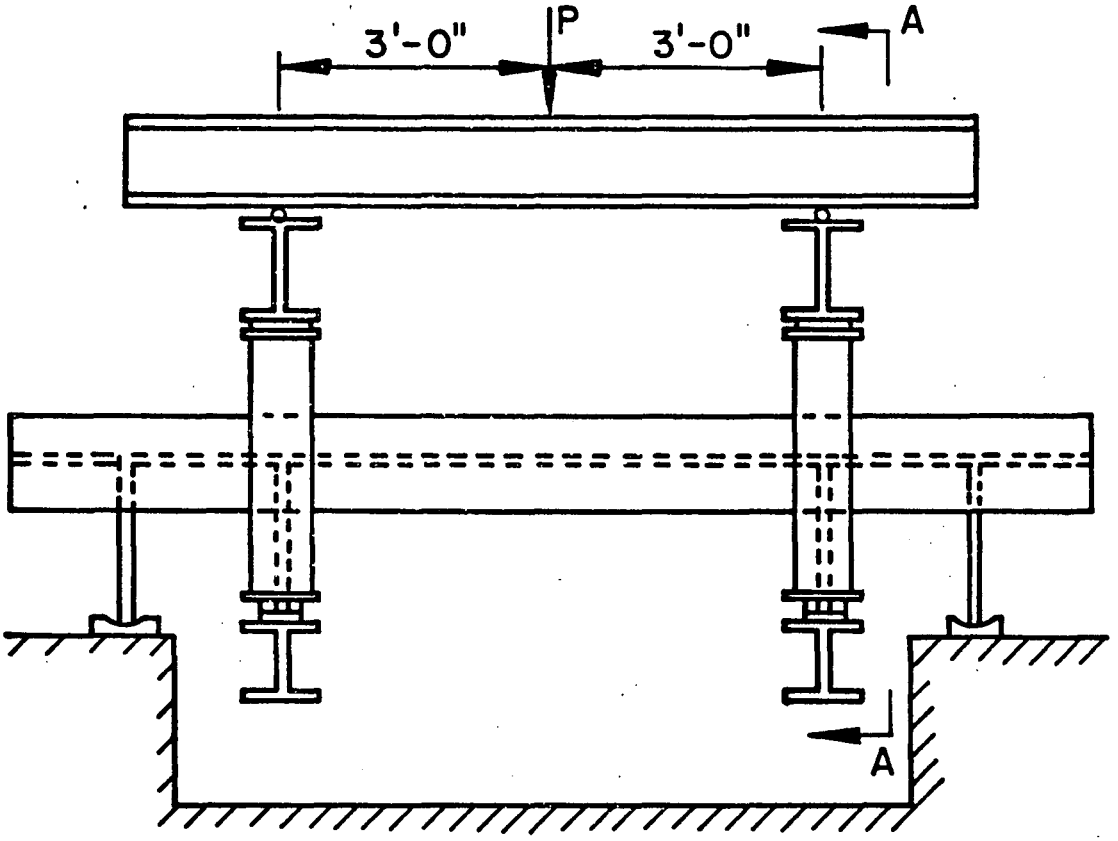

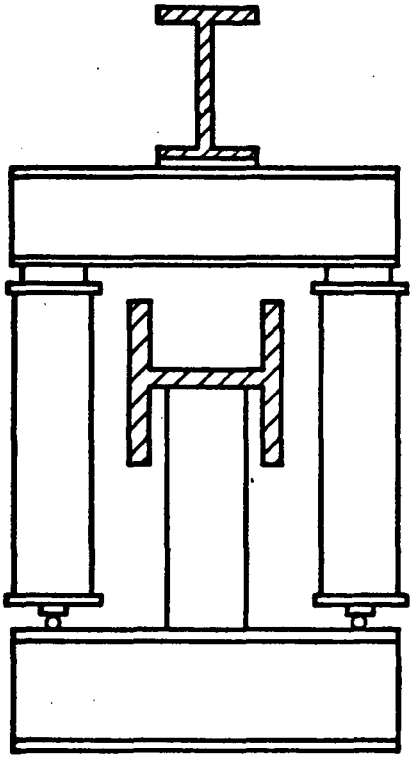

Section A-A

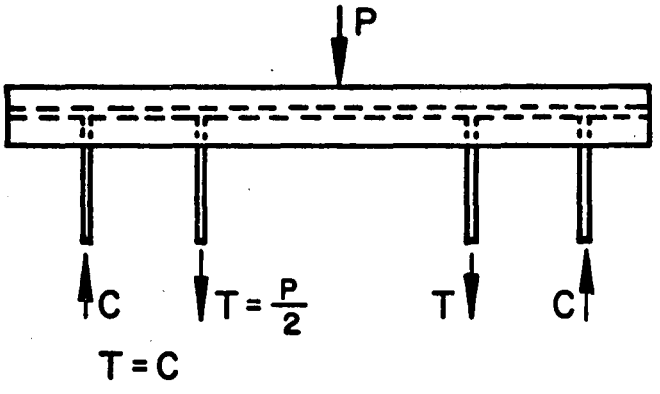

Schematic Diagram

Fig. 4 Pilot Test Setup

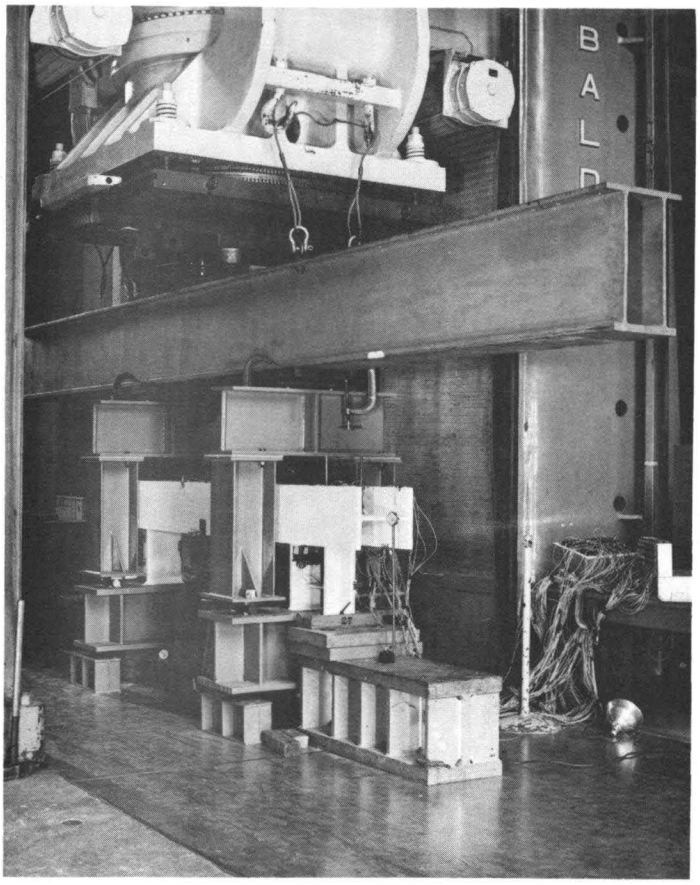

Fig. 5 Pilot Test Setup

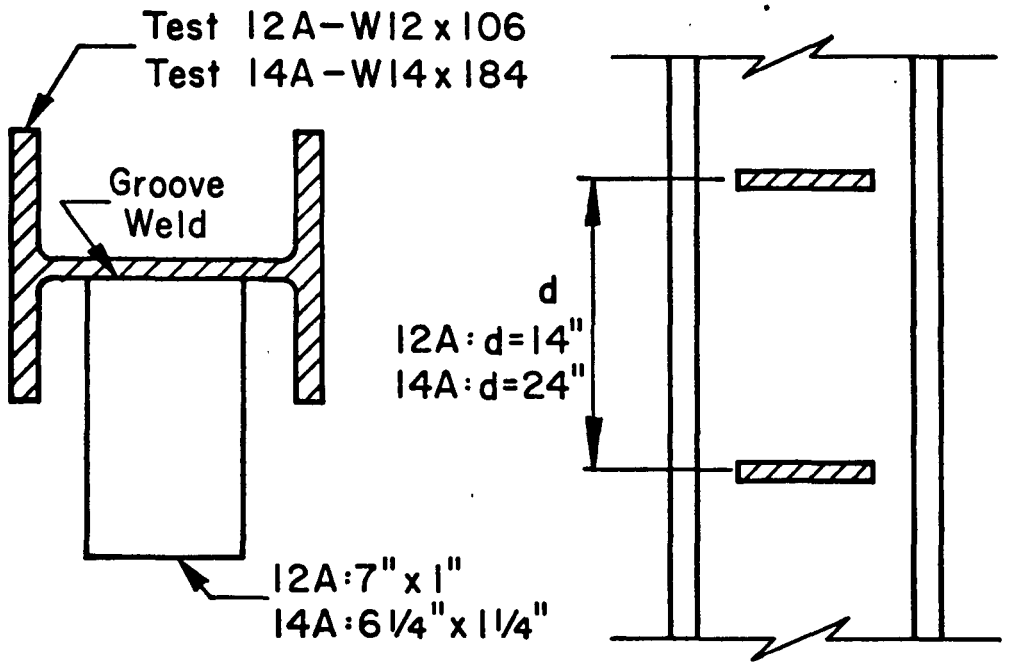

Test A

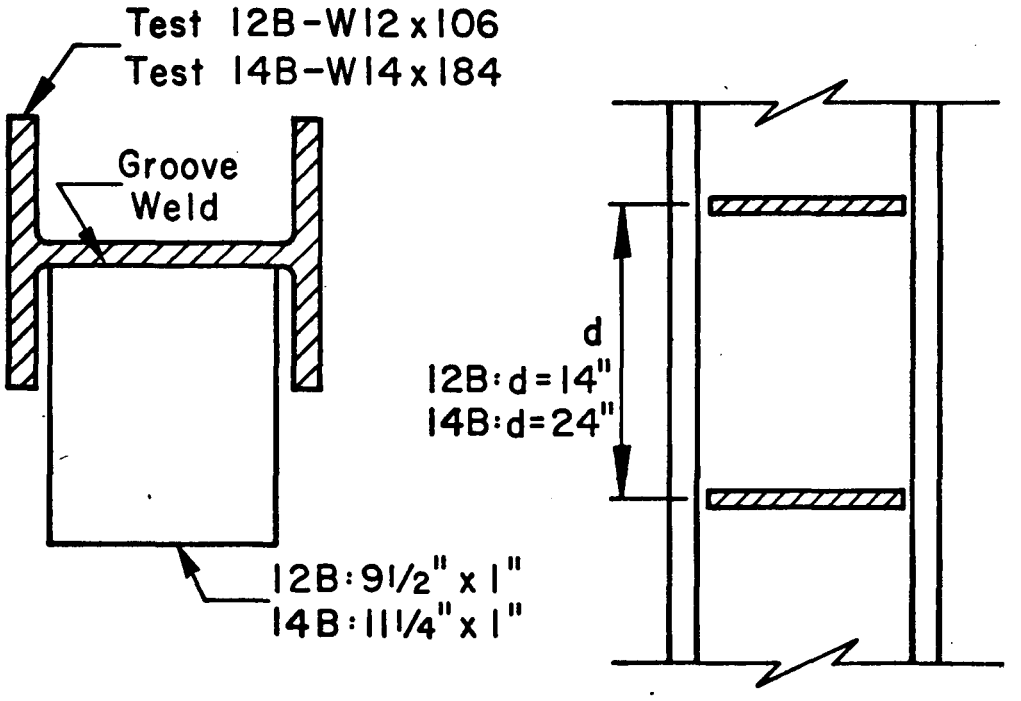

Test B

Fig. 6 Pilot Tests A and B

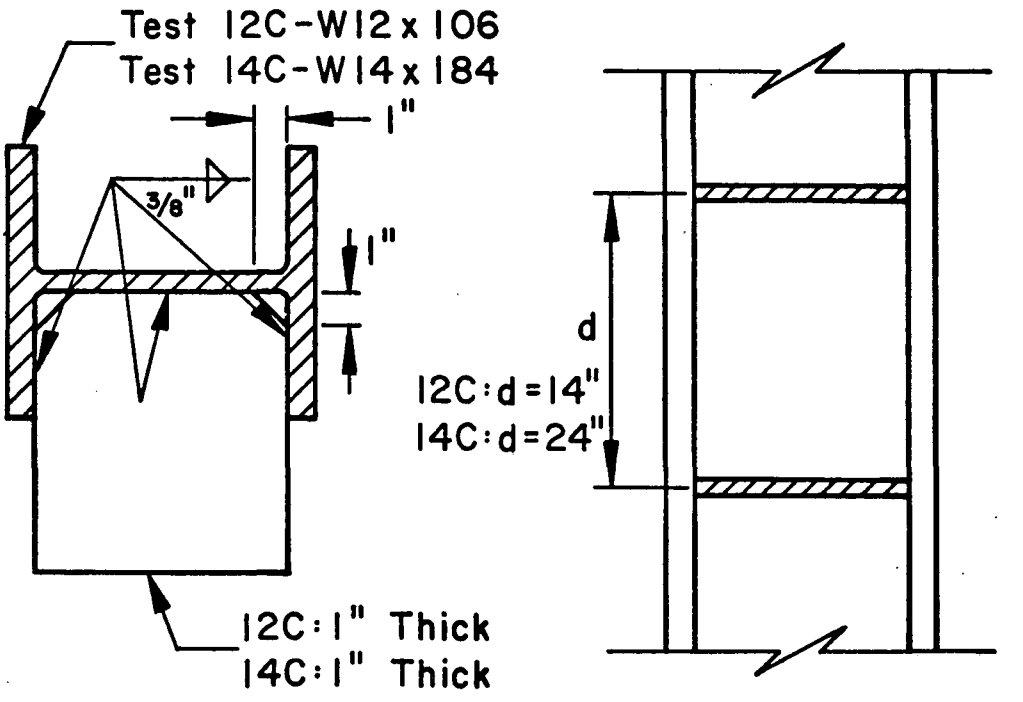

Test C

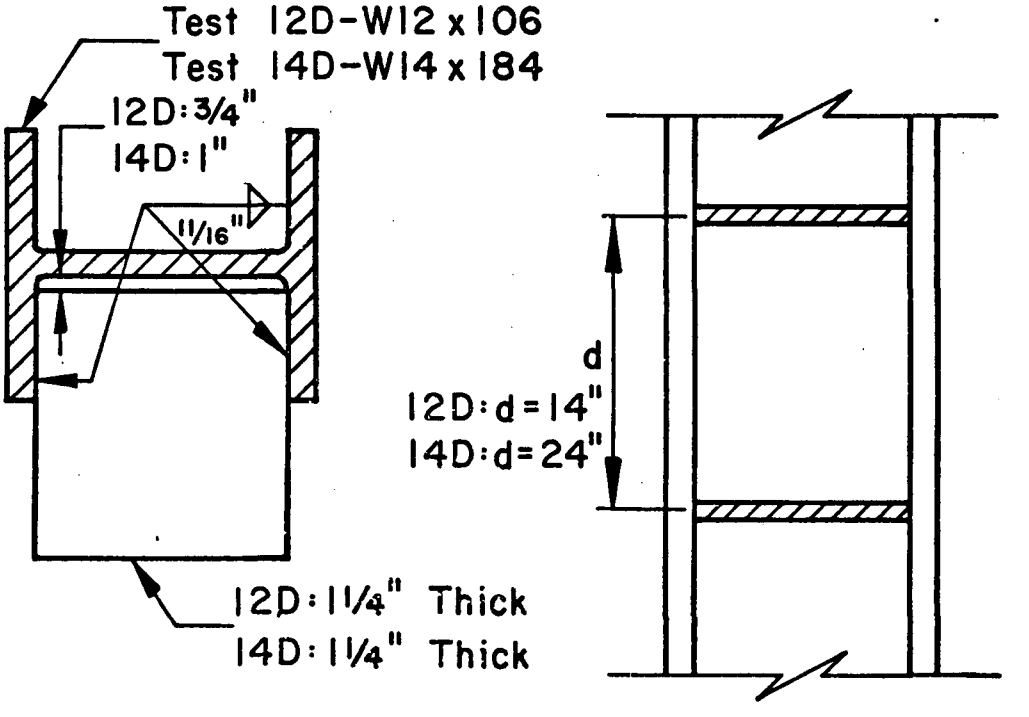

Test D

Fig. 7 Pilot Tests C and D

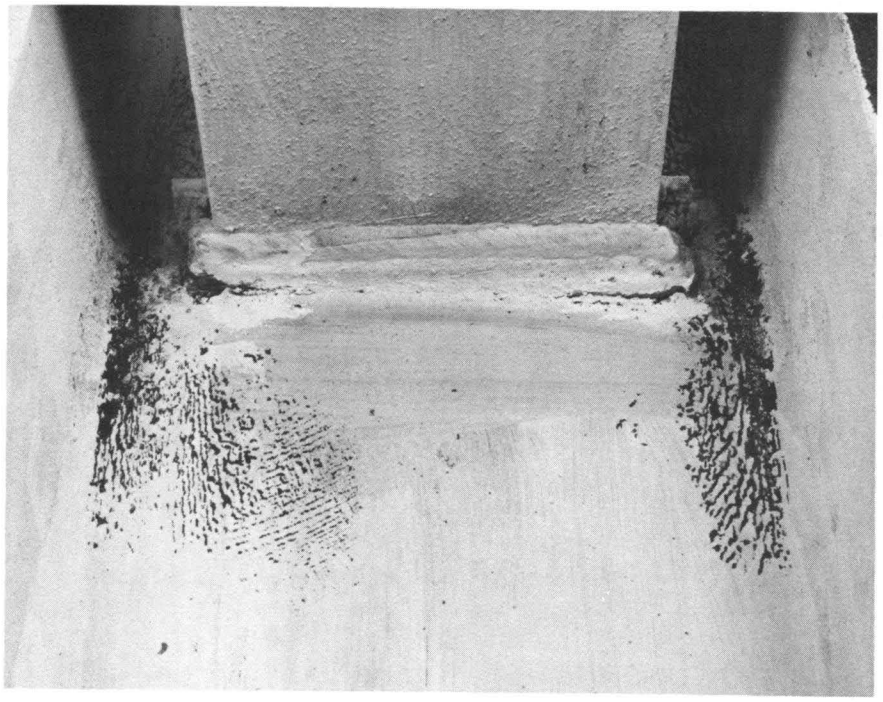

Fig. 8 Test 12A Column Web at Tension Plate

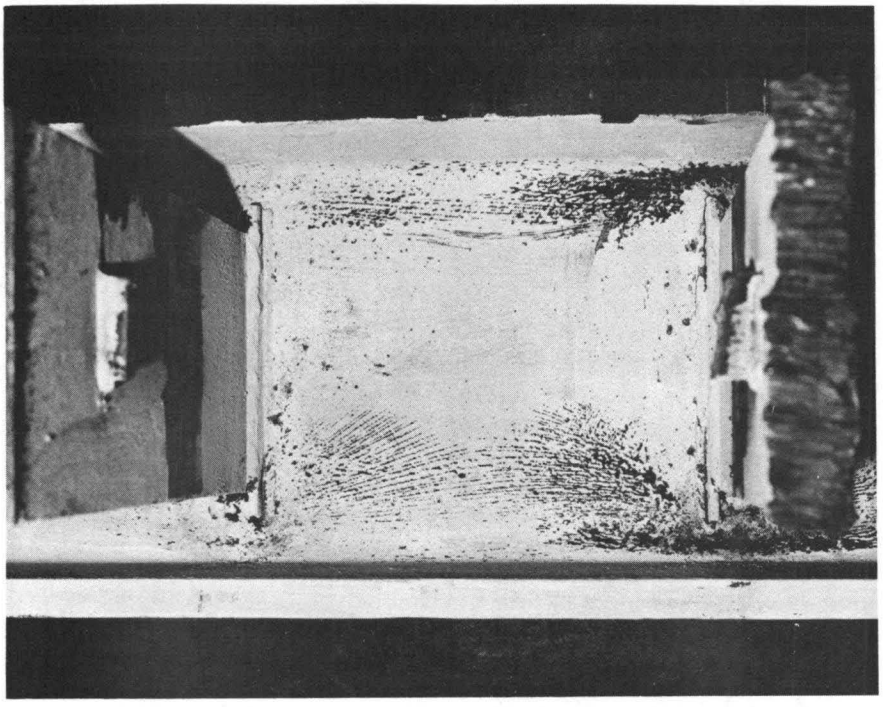

Fig. 9 Pilot Test 12A Web Panel Zone

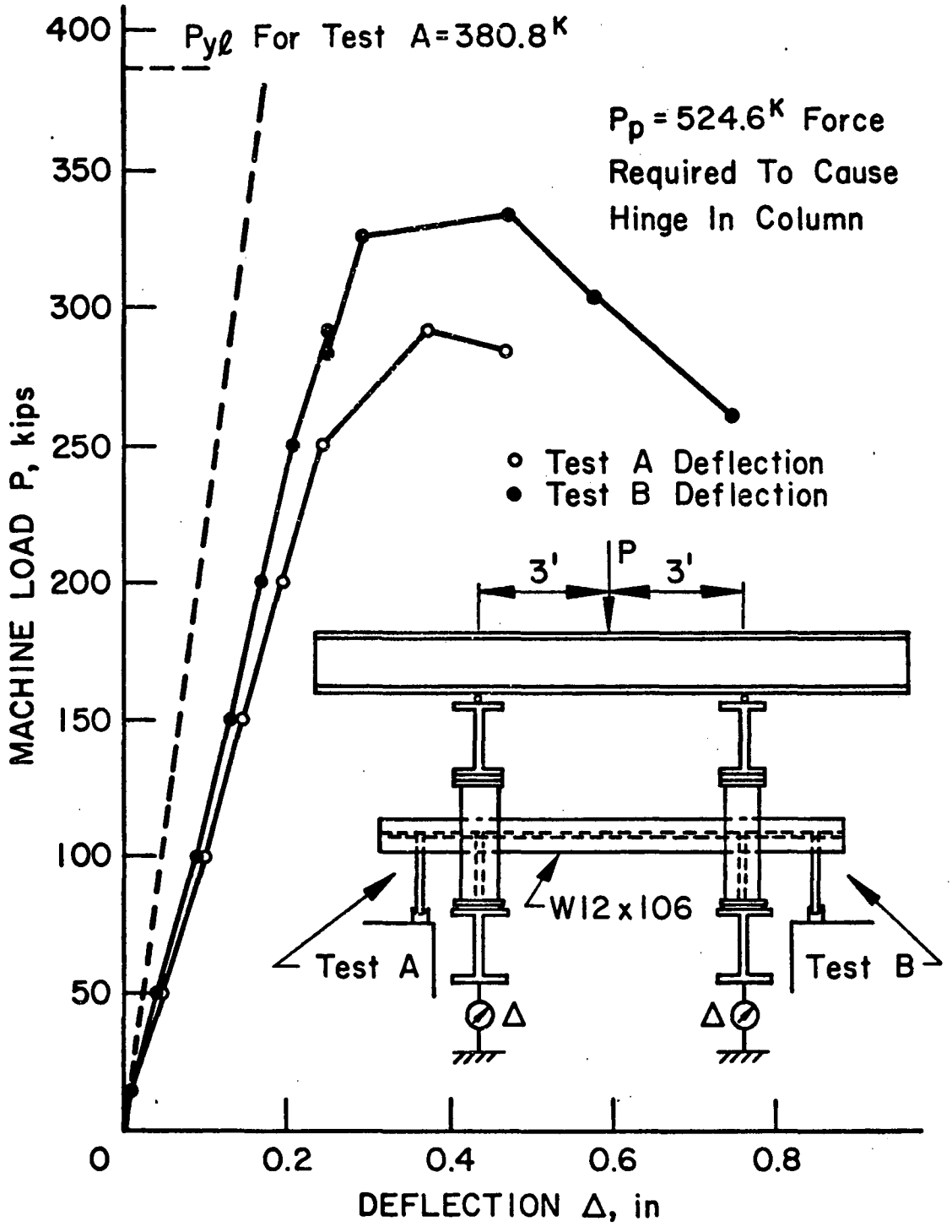

Fig. 10 Tension Plate Deflection for 12A and 12B

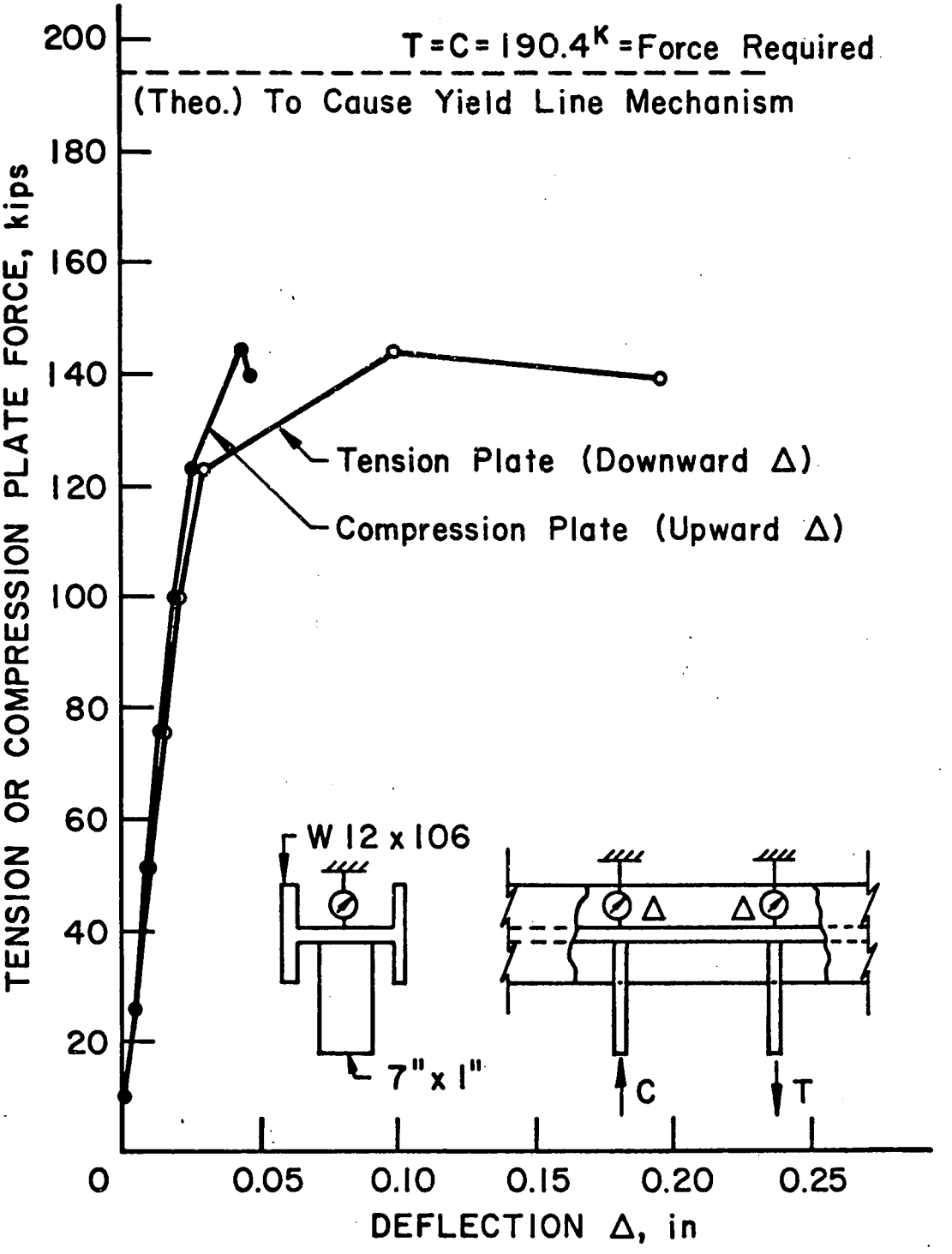

Fig. 11 Column Web Deflection for Test 12A

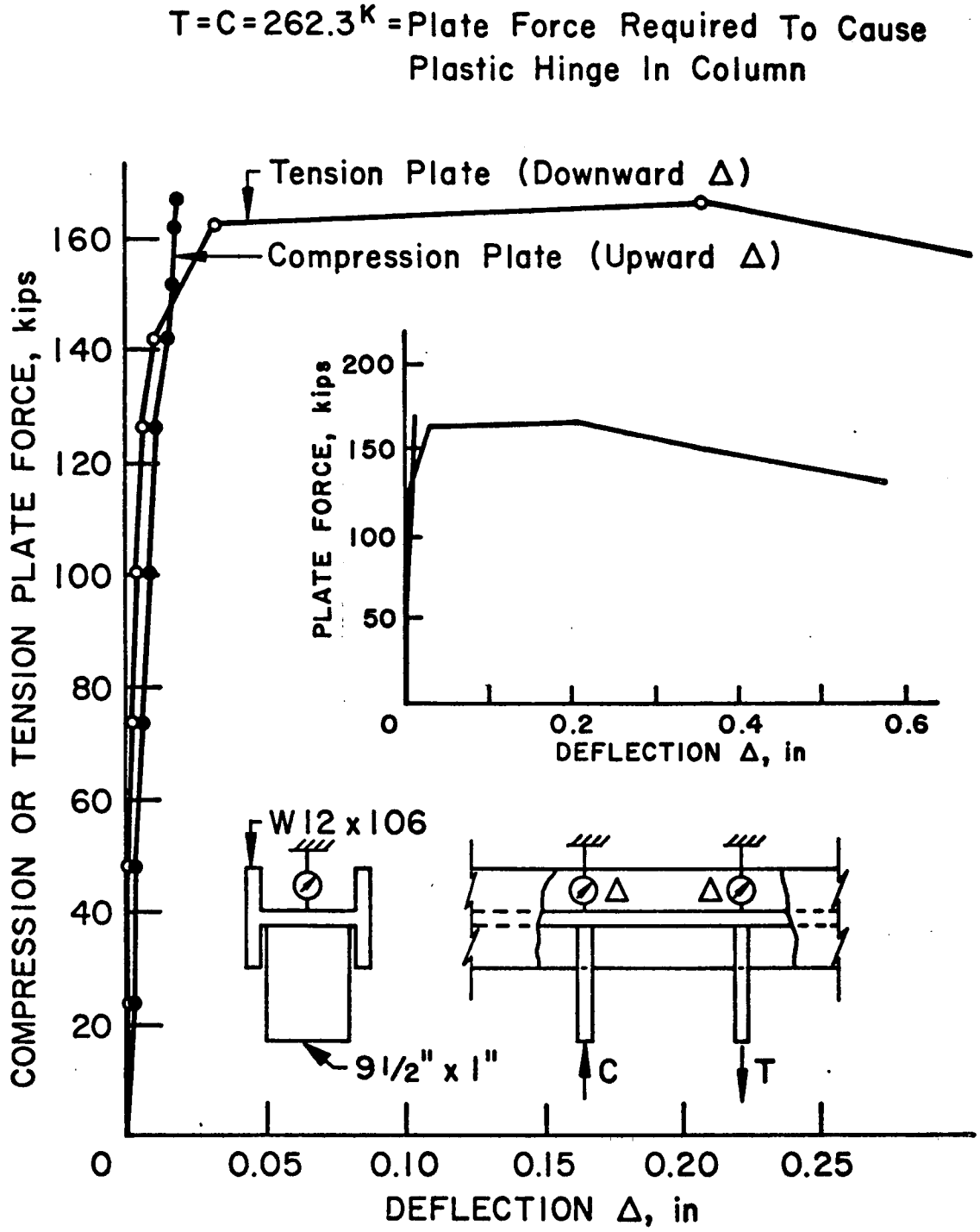

Fig. 12 Column Web Deflection for Test 12B

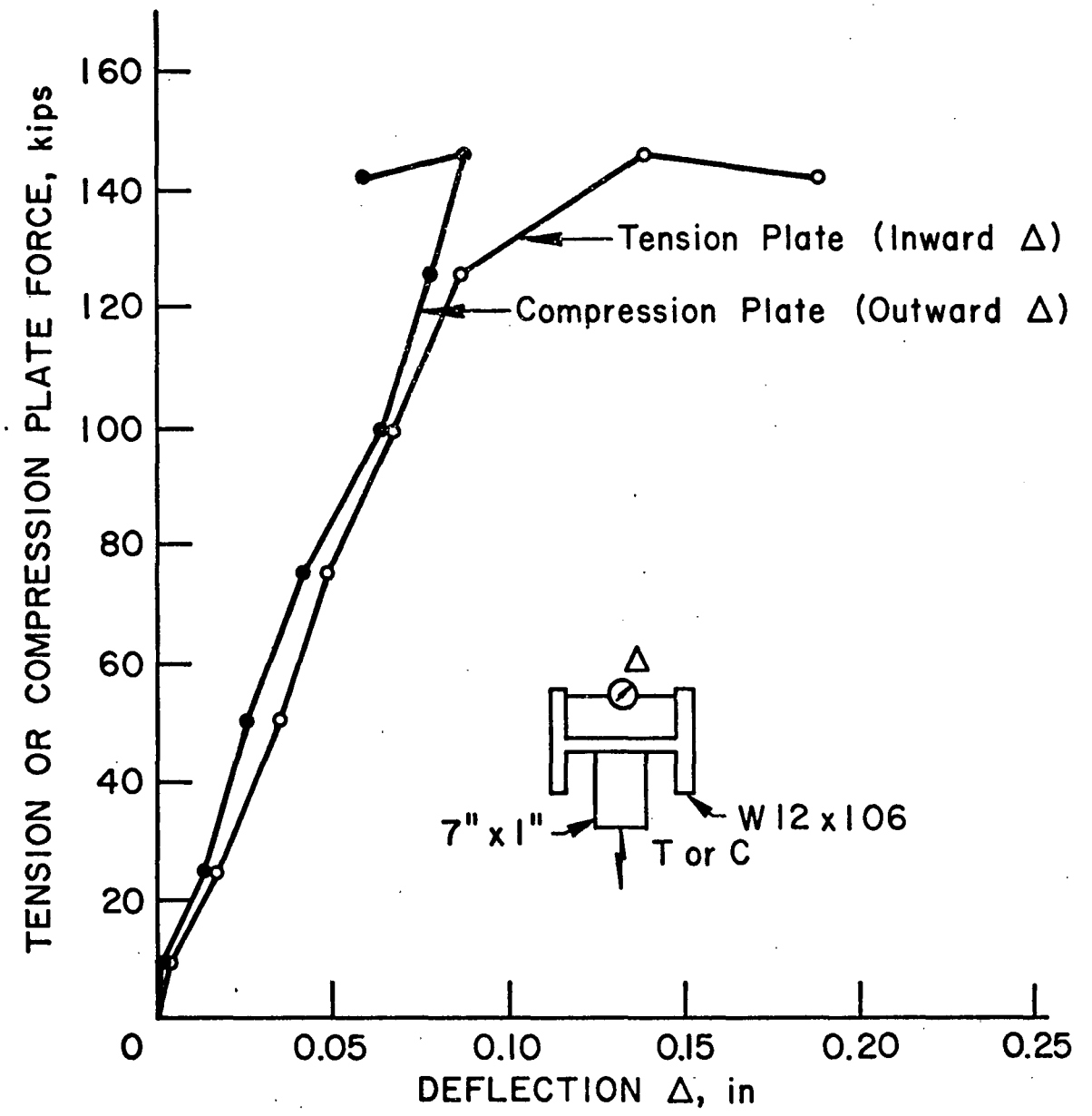

Fig. 13 Column Flange Movement for Test 12A

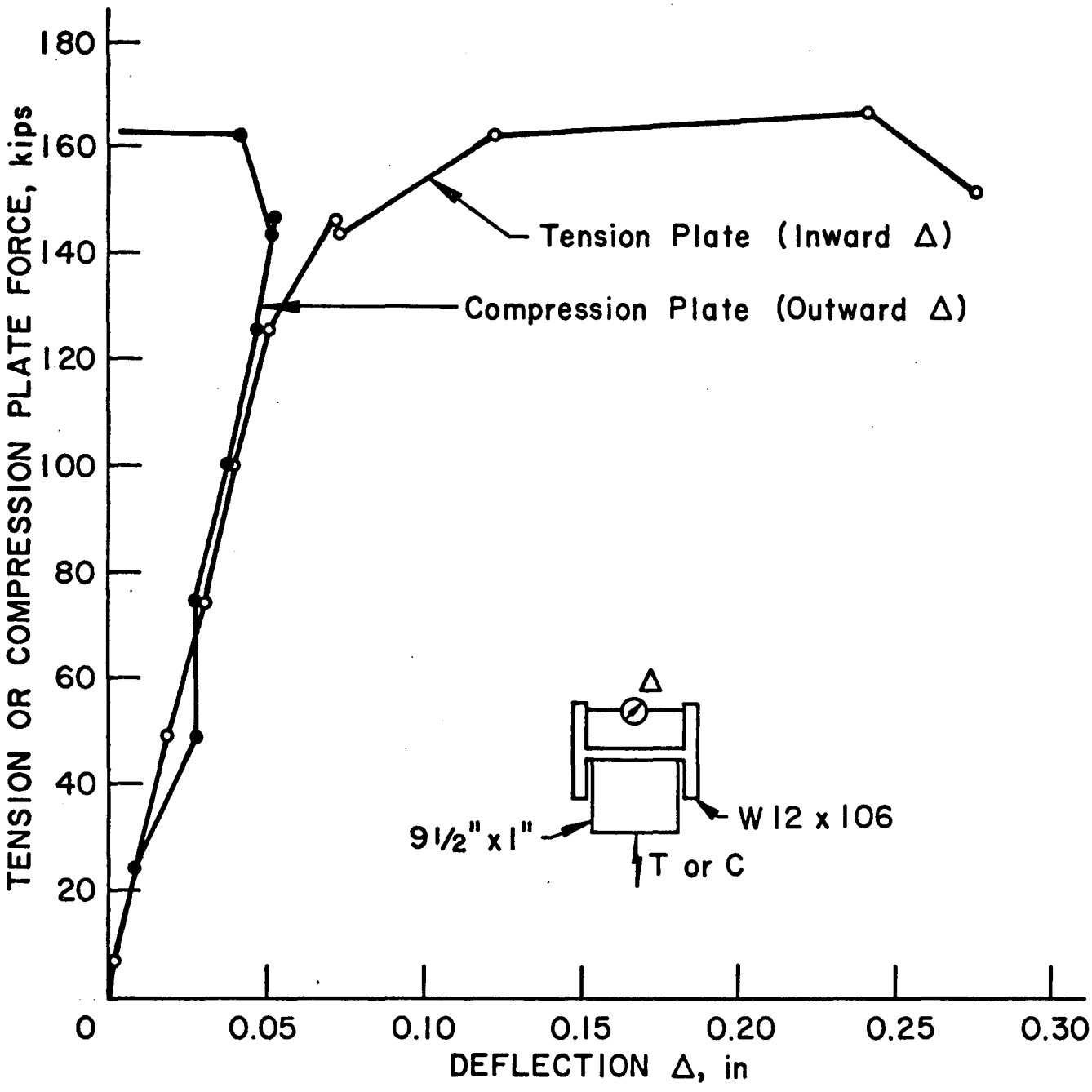

Fig. 14 Column Flange Movement for Test 12B

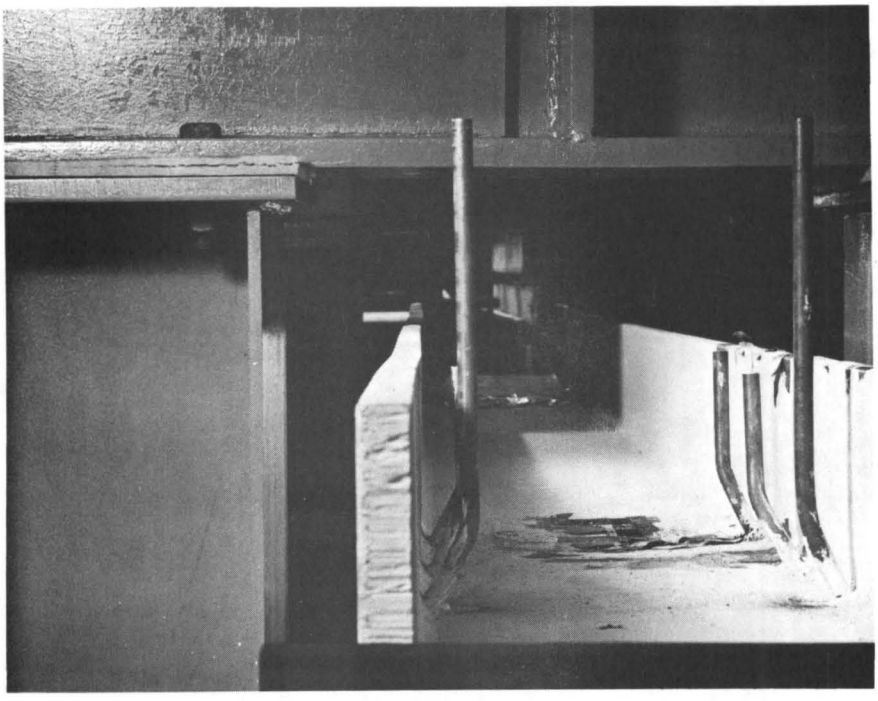

Fig. 15 Test 12A Column Flange Movement

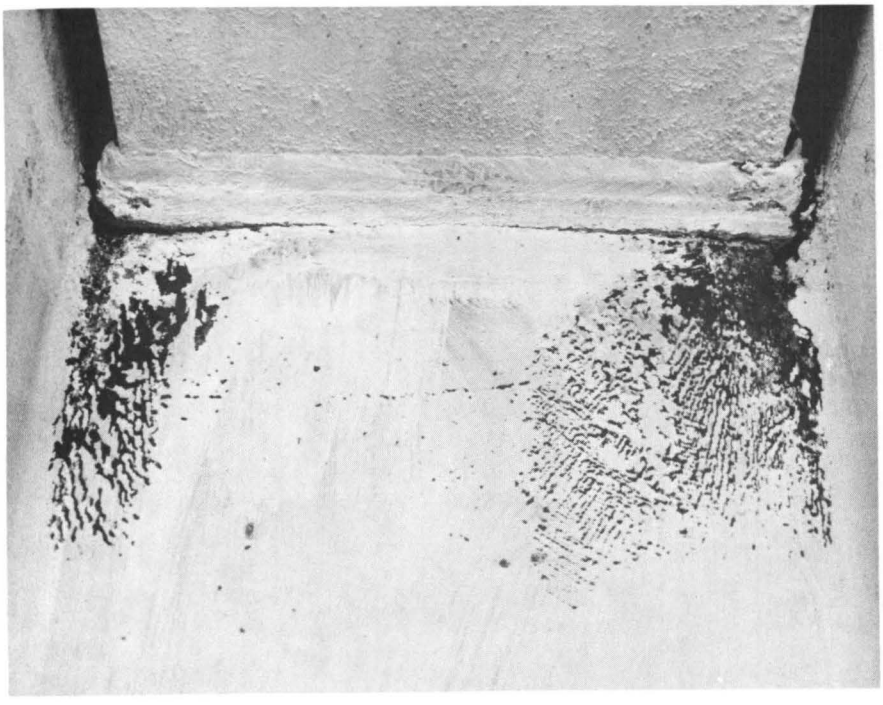

Fig. 16 Test 12B Column Web at Tension Plate

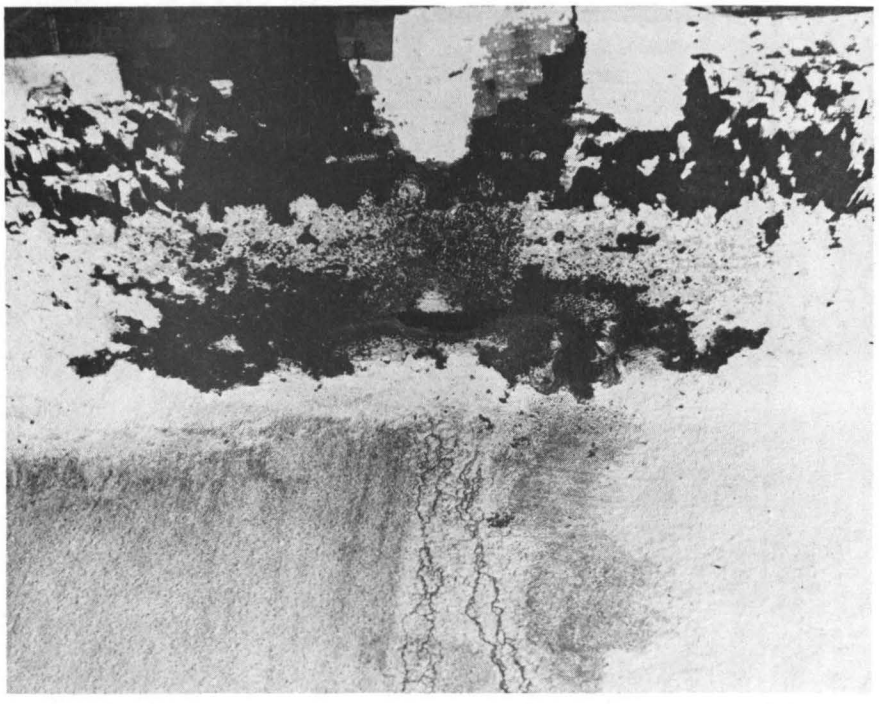

Fig. 17 Web Fracture Opposite Test 12B Tension Plate

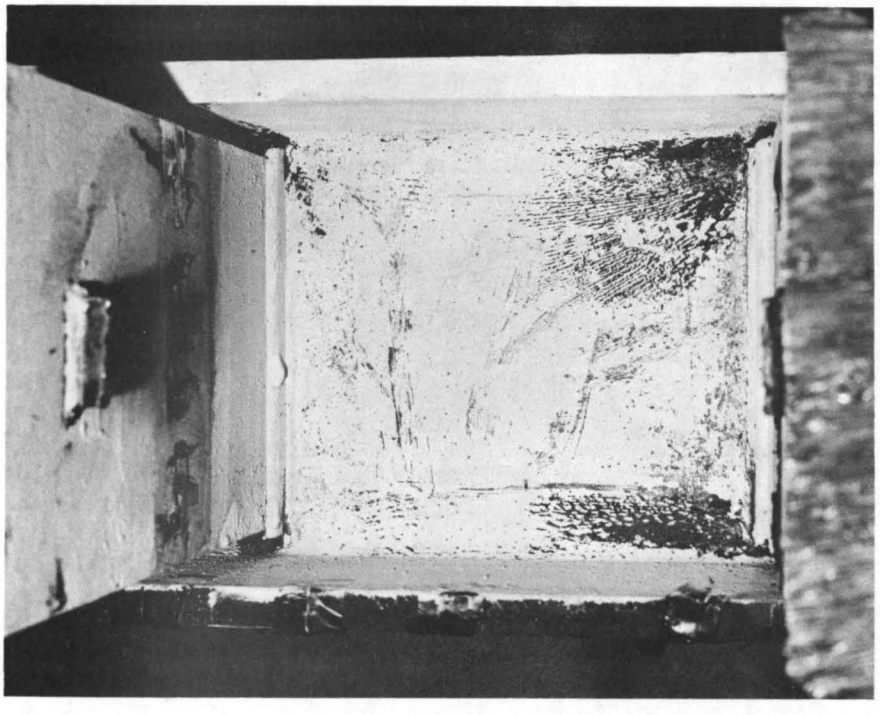

Fig. 18 Pilot Test 12B Web Panel Zone

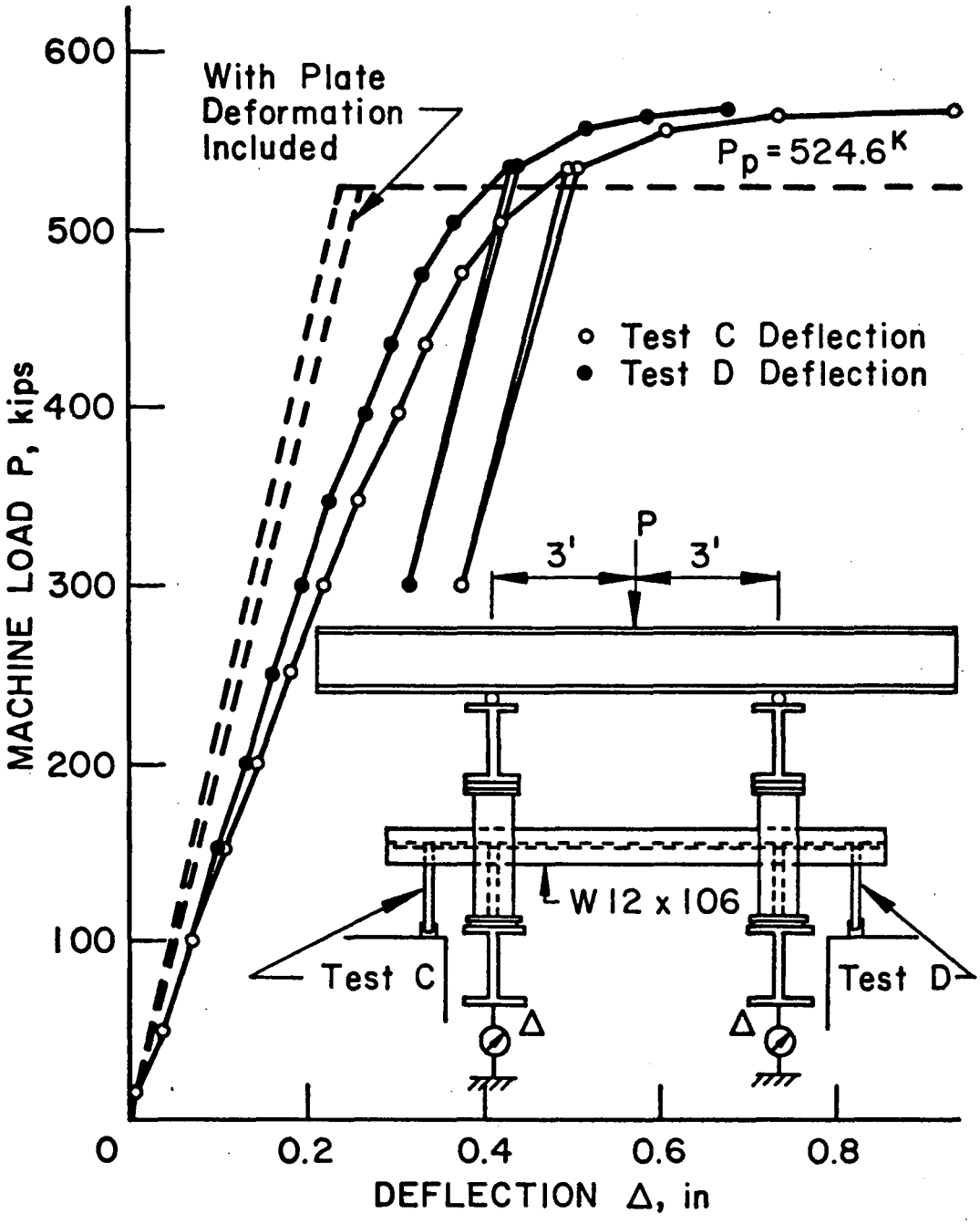

Fig. 19 Tension Plate Deflection for 12C and 12D

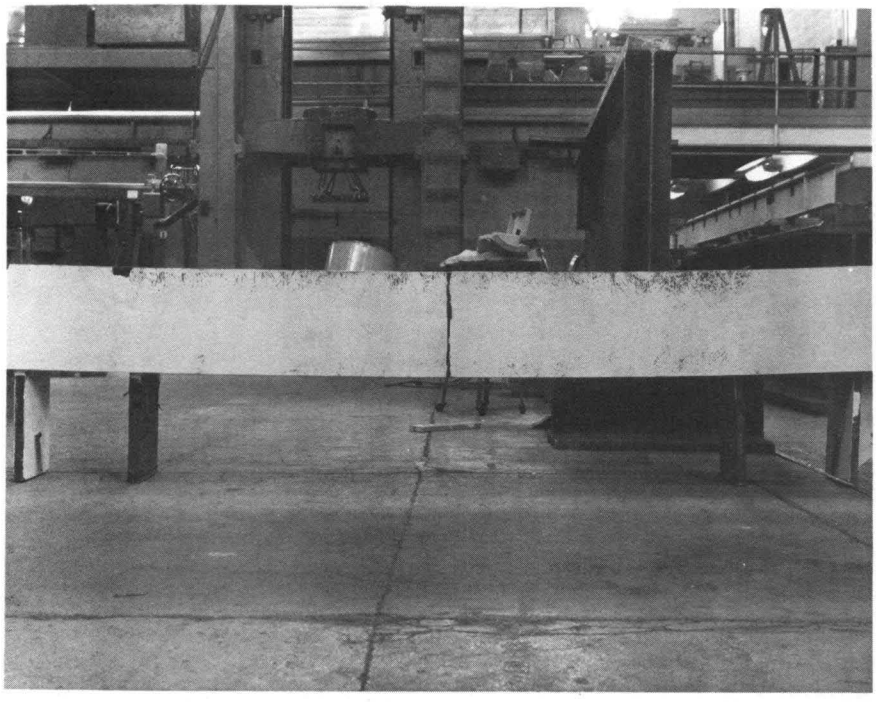

Fig. 20 Test 12C and 12D After Testing

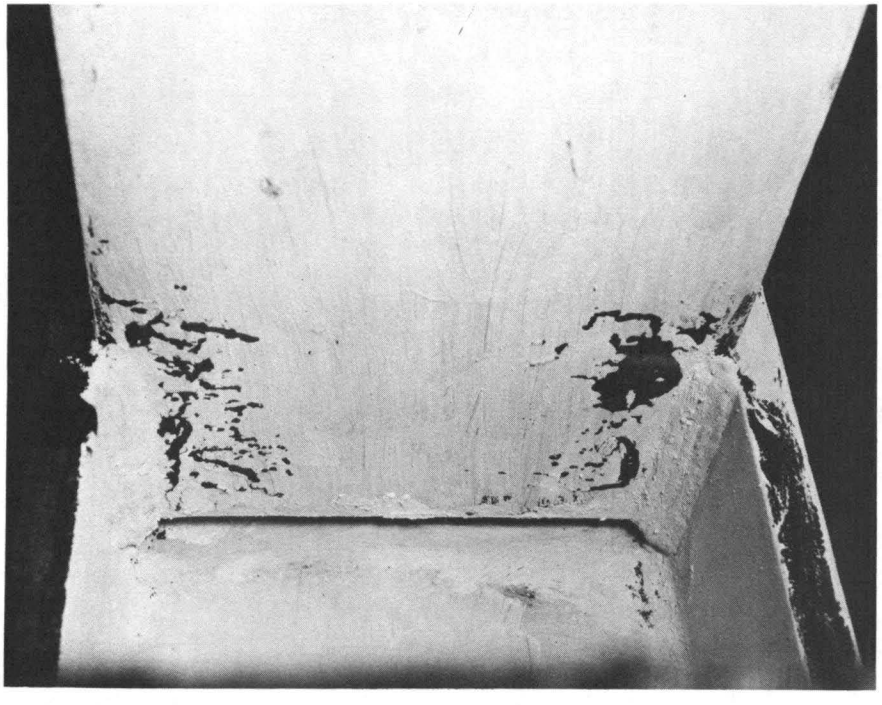

Fig. 21 Test 12D Compression Plate Shear Yielding

Fig. 22 Test 14A Column Web at Tension Plate

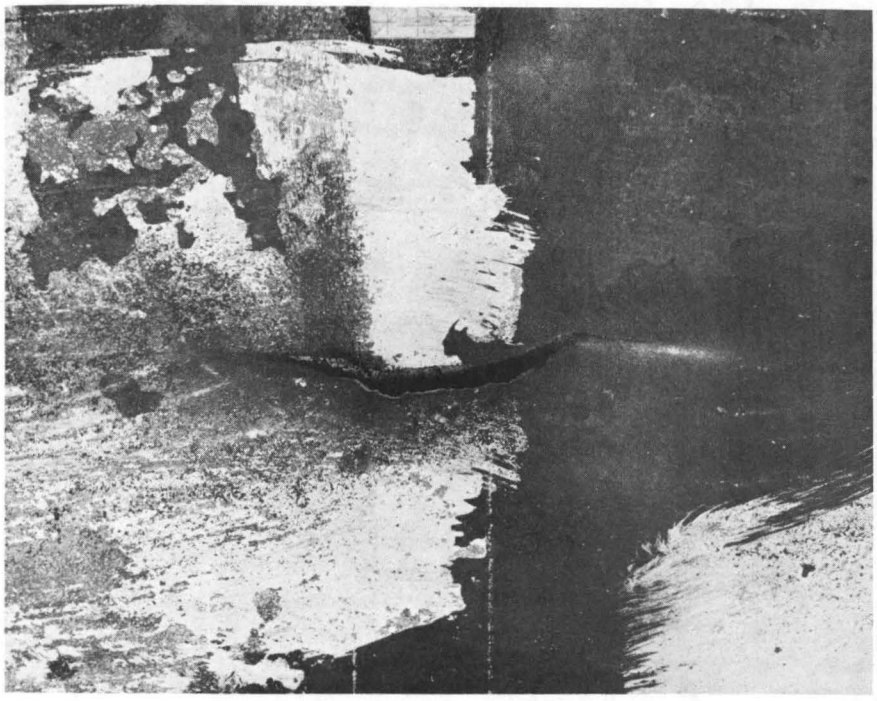

Fig. 23 Web Fracture Opposite Test 14A Tension Plate

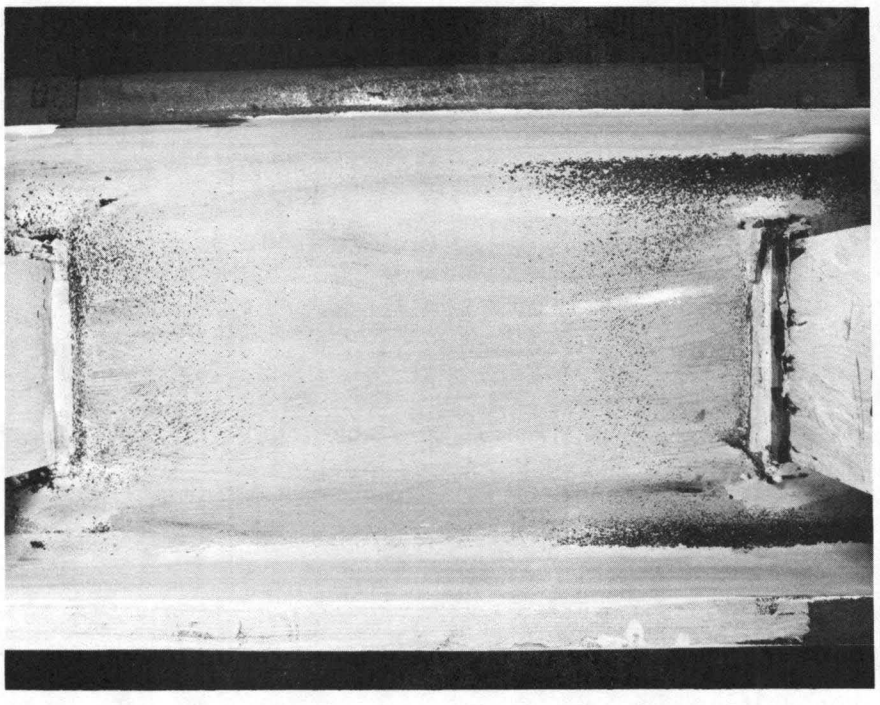

Fig. 24 Pilot Test 14A Web Panel Zone

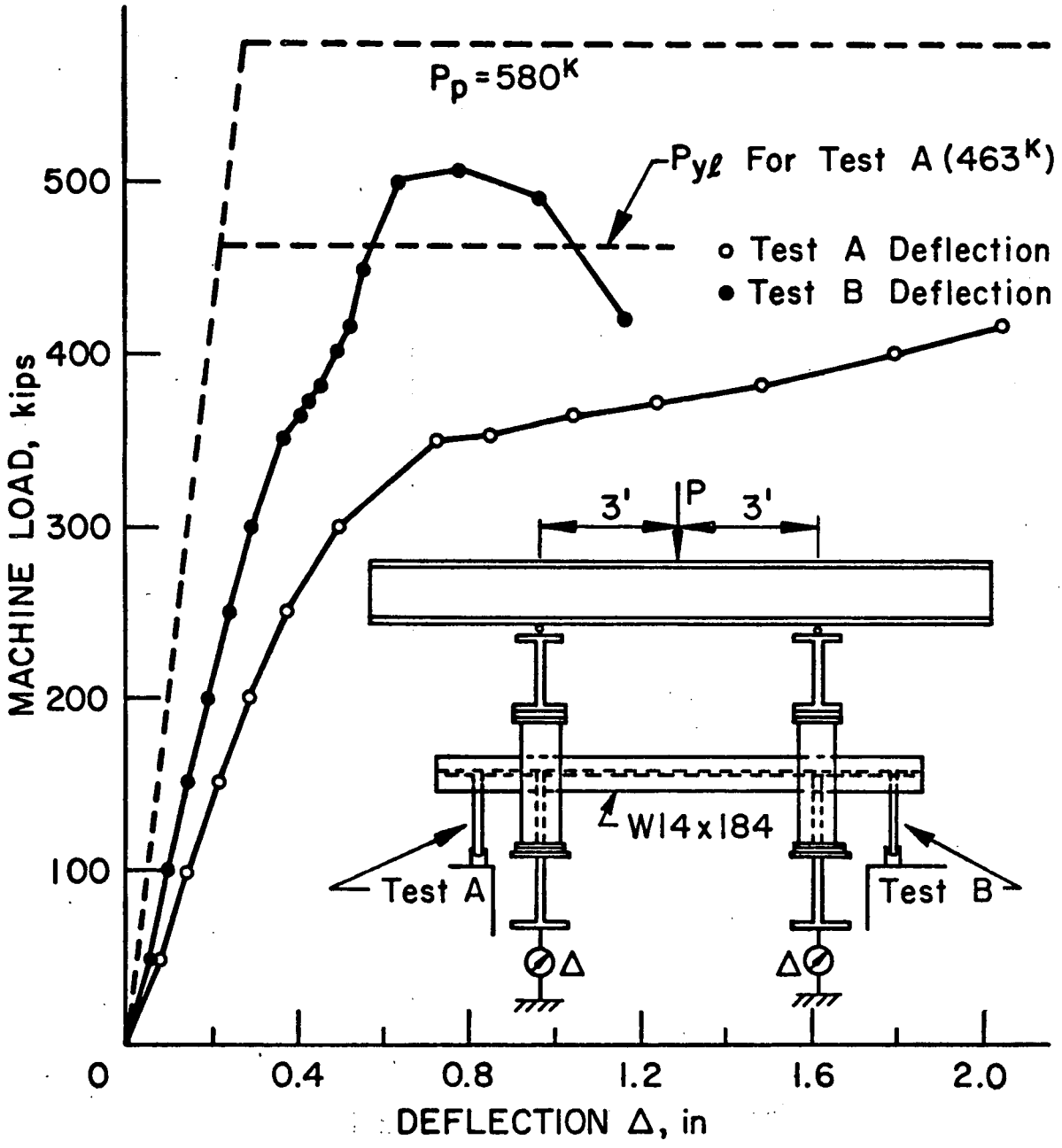

Fig. 25 Tests 14A and 14B Tension Plate Deflections

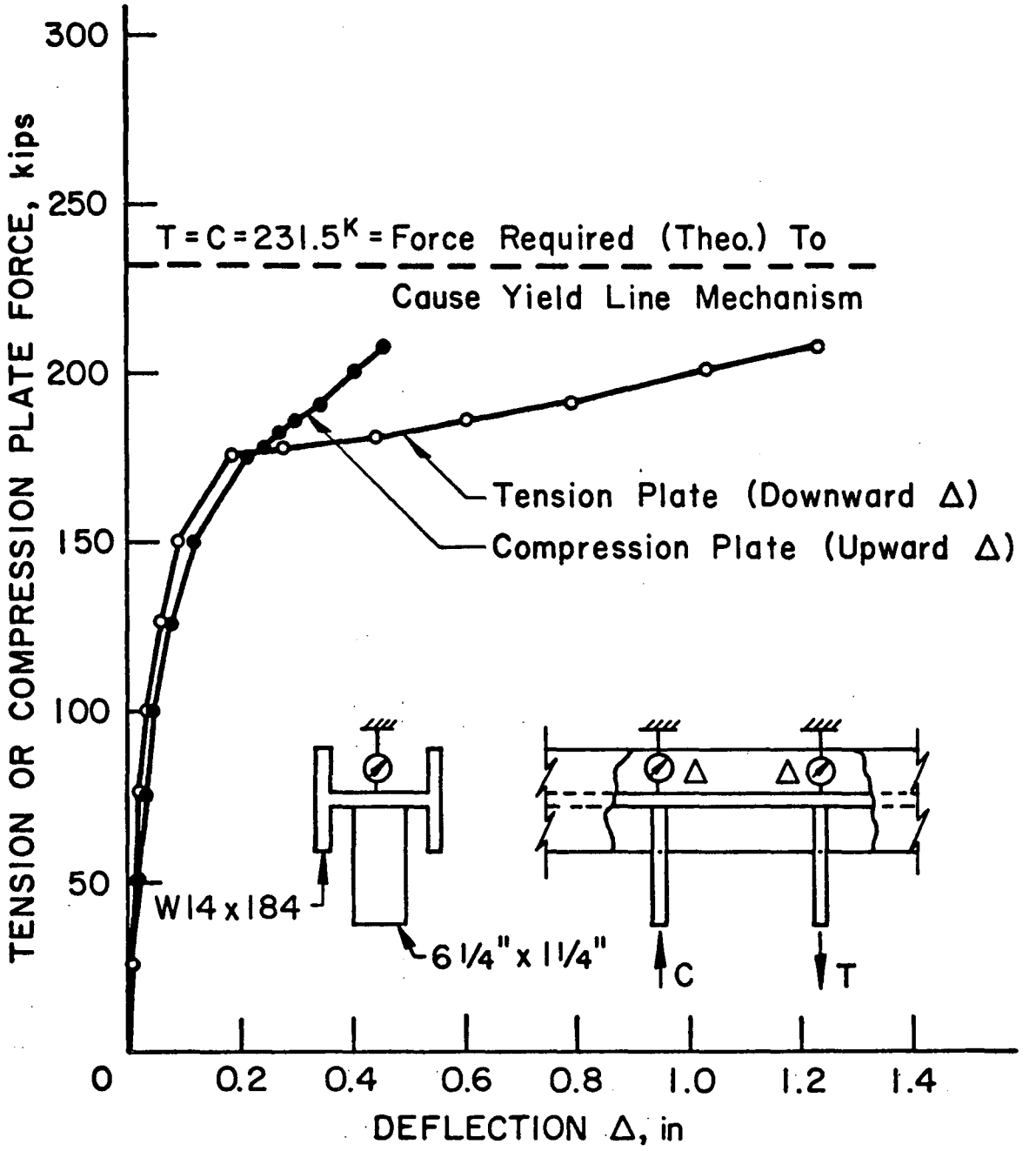

Fig. 26 Test 14A Column Web Deflection

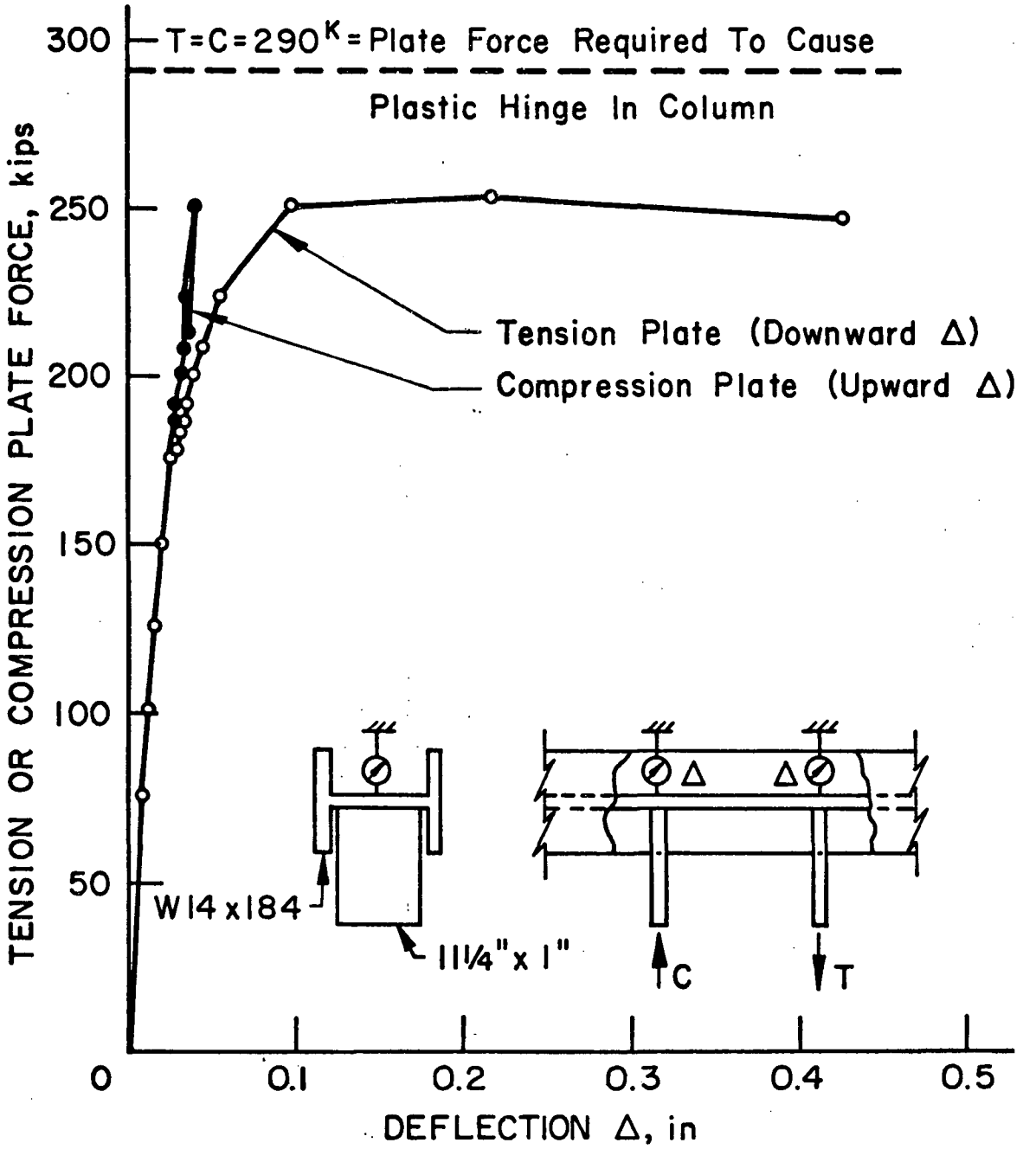

Fig. 27 Test 14B Column Web Deflection

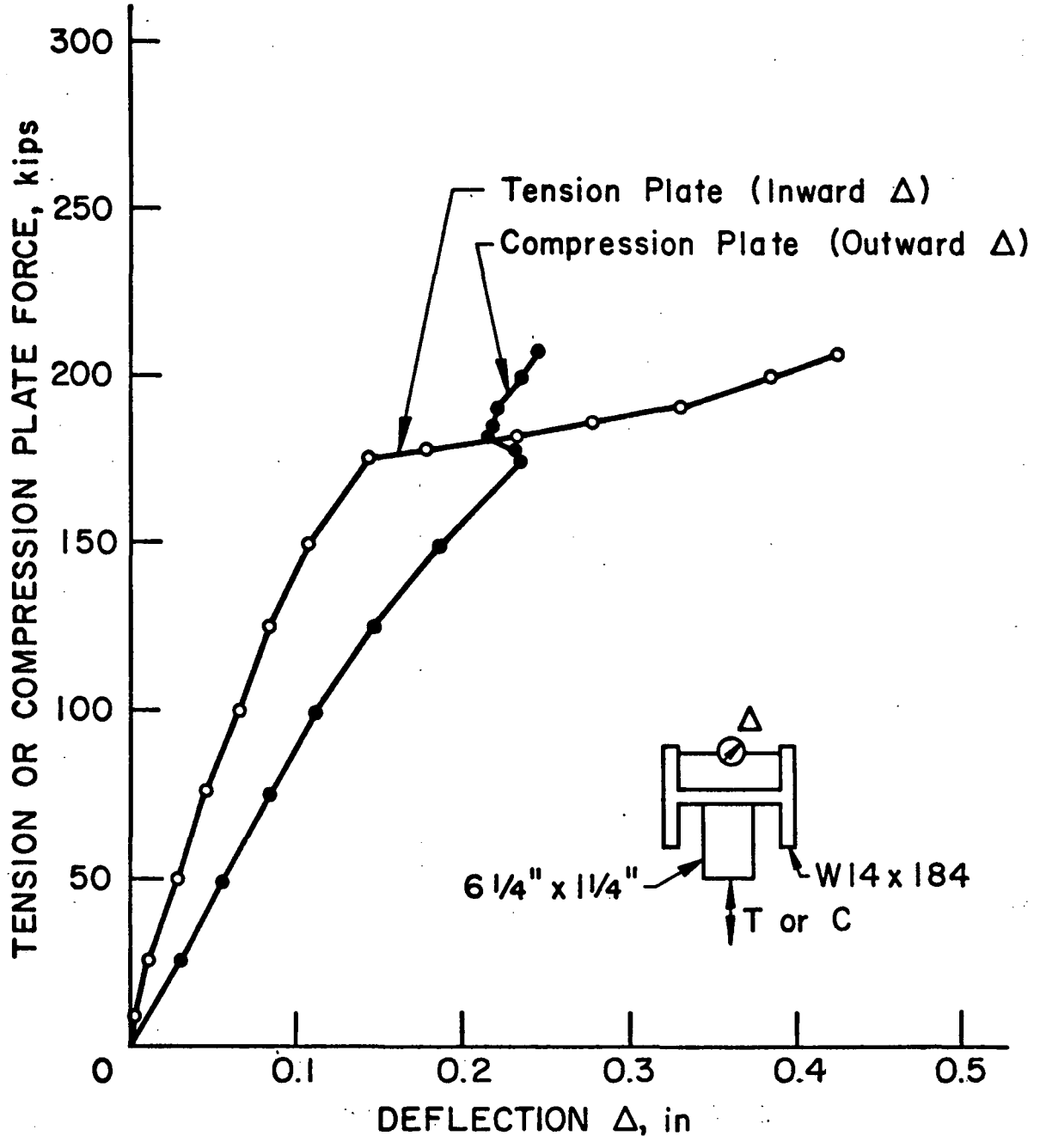

Fig. 28 Test 14A Column Flange Movement

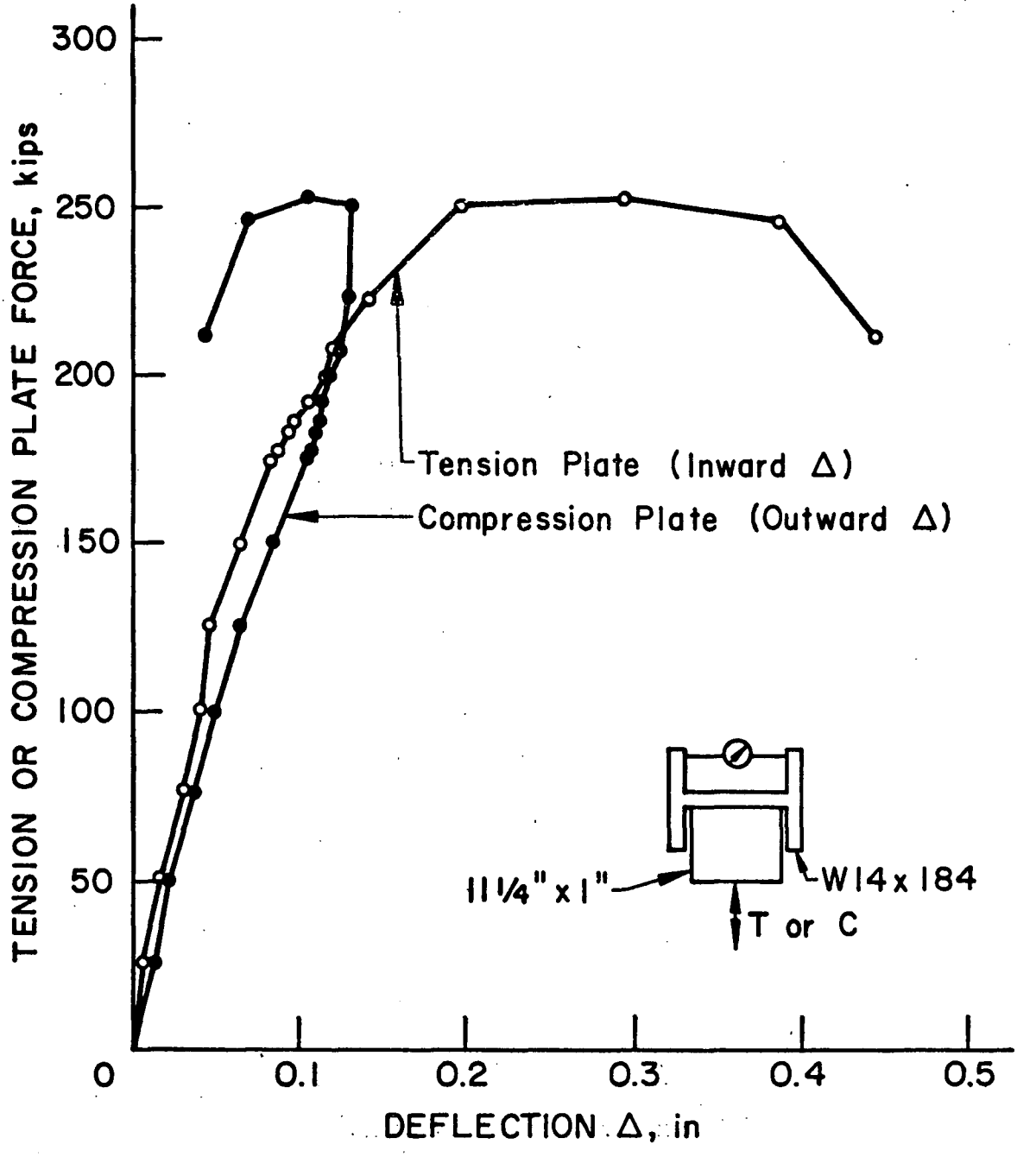

Fig. 29 Test 14B Column Flange Movement

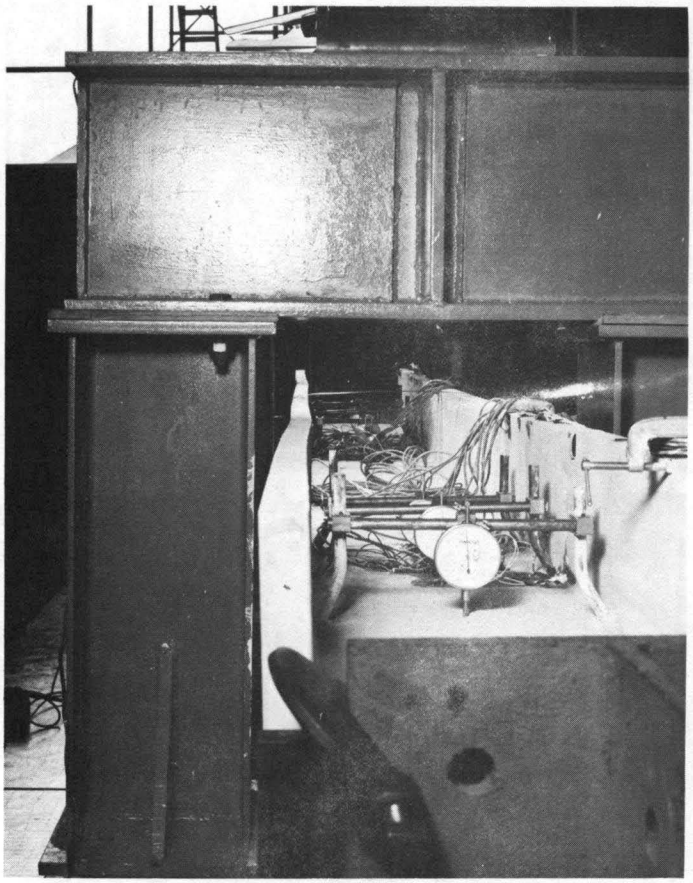

Fig. 30 Tests 14A and 14B Column Flange Movement

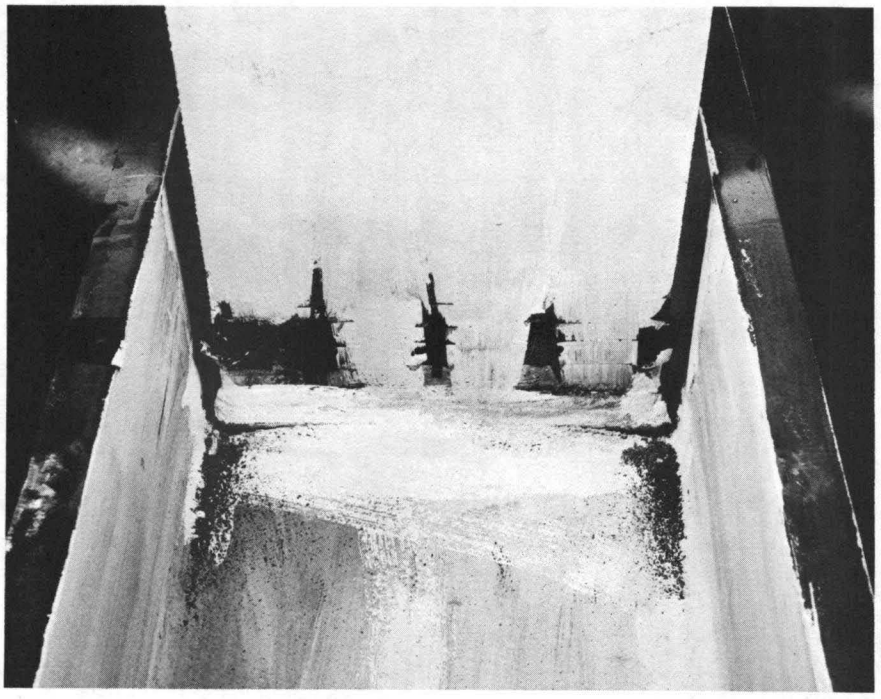

Fig. 31 Test 14B Column Web at Tension Plate

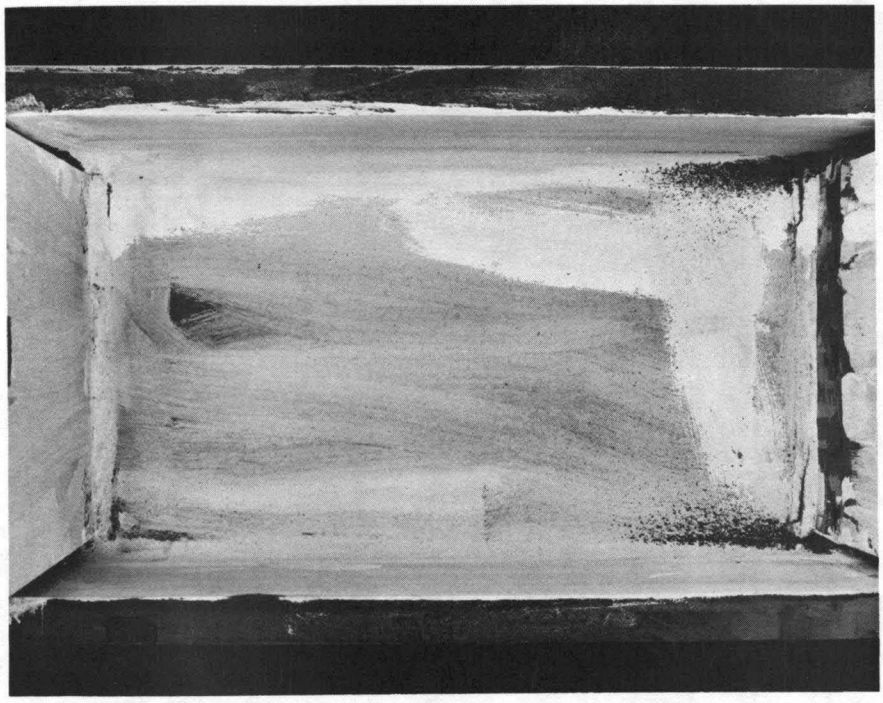

Fig. 32 Pilot Test 14B Web Panel Zone

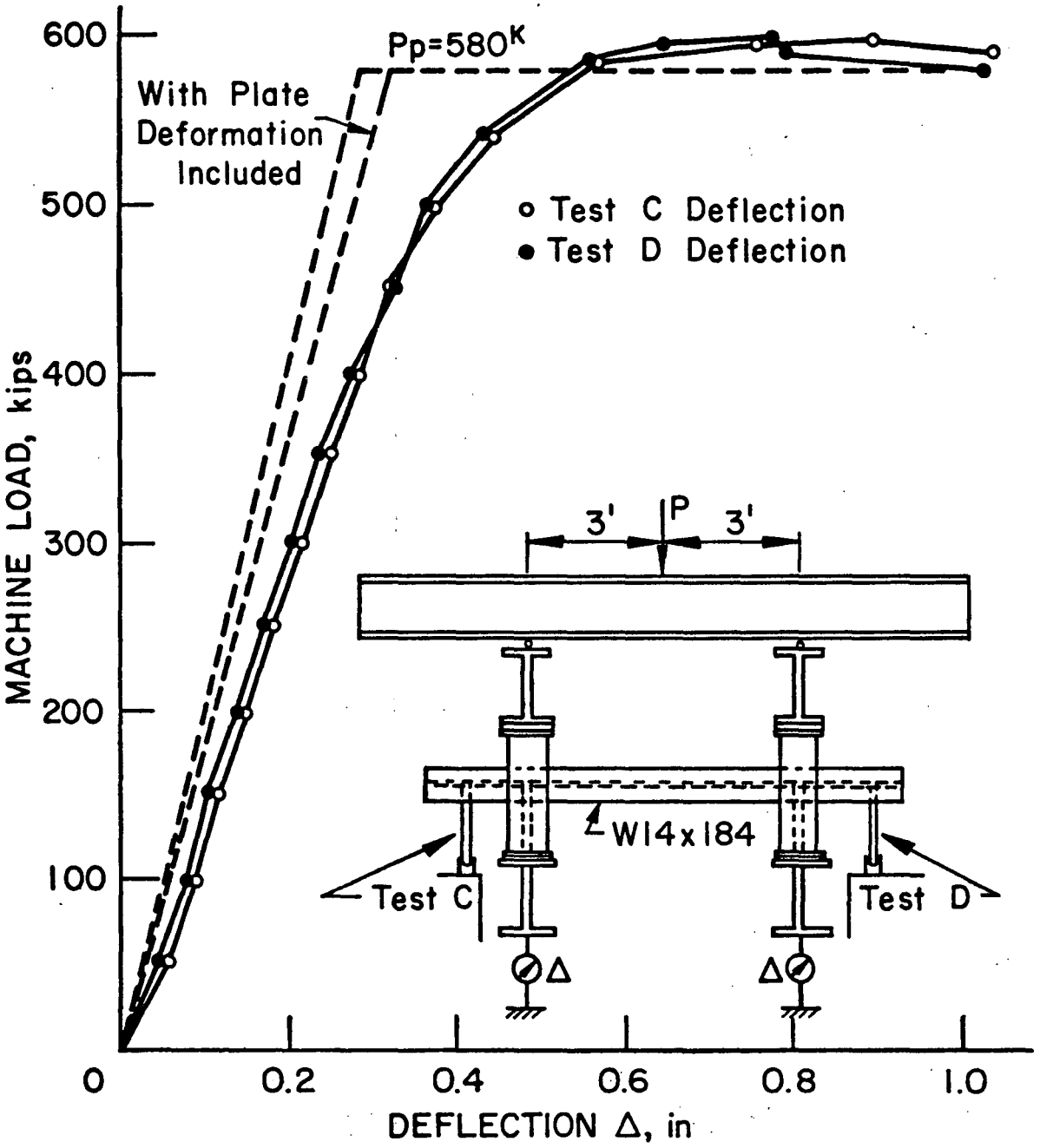

Fig. 33 Tests 14C and 14D Tension Plate Deflections

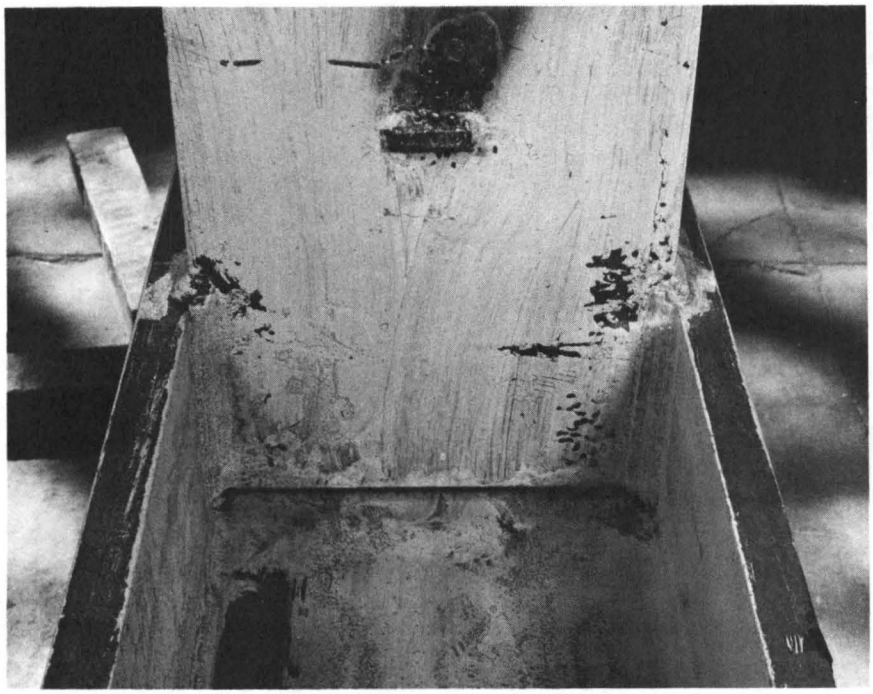

Fig. 34 Test 14D Compression Plate Shear Yielding

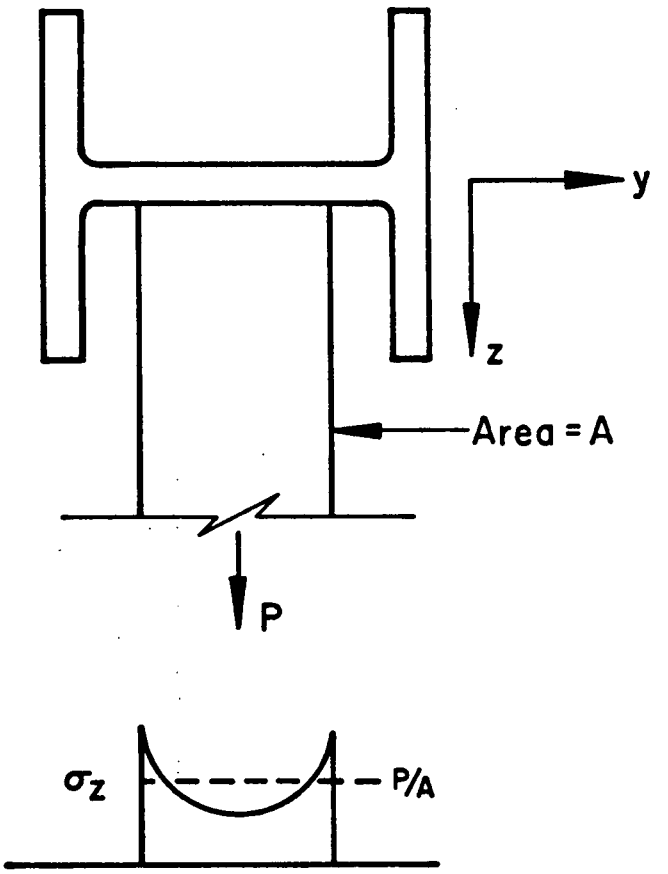

Fig. 35 Stress Distribution in Tension Plate

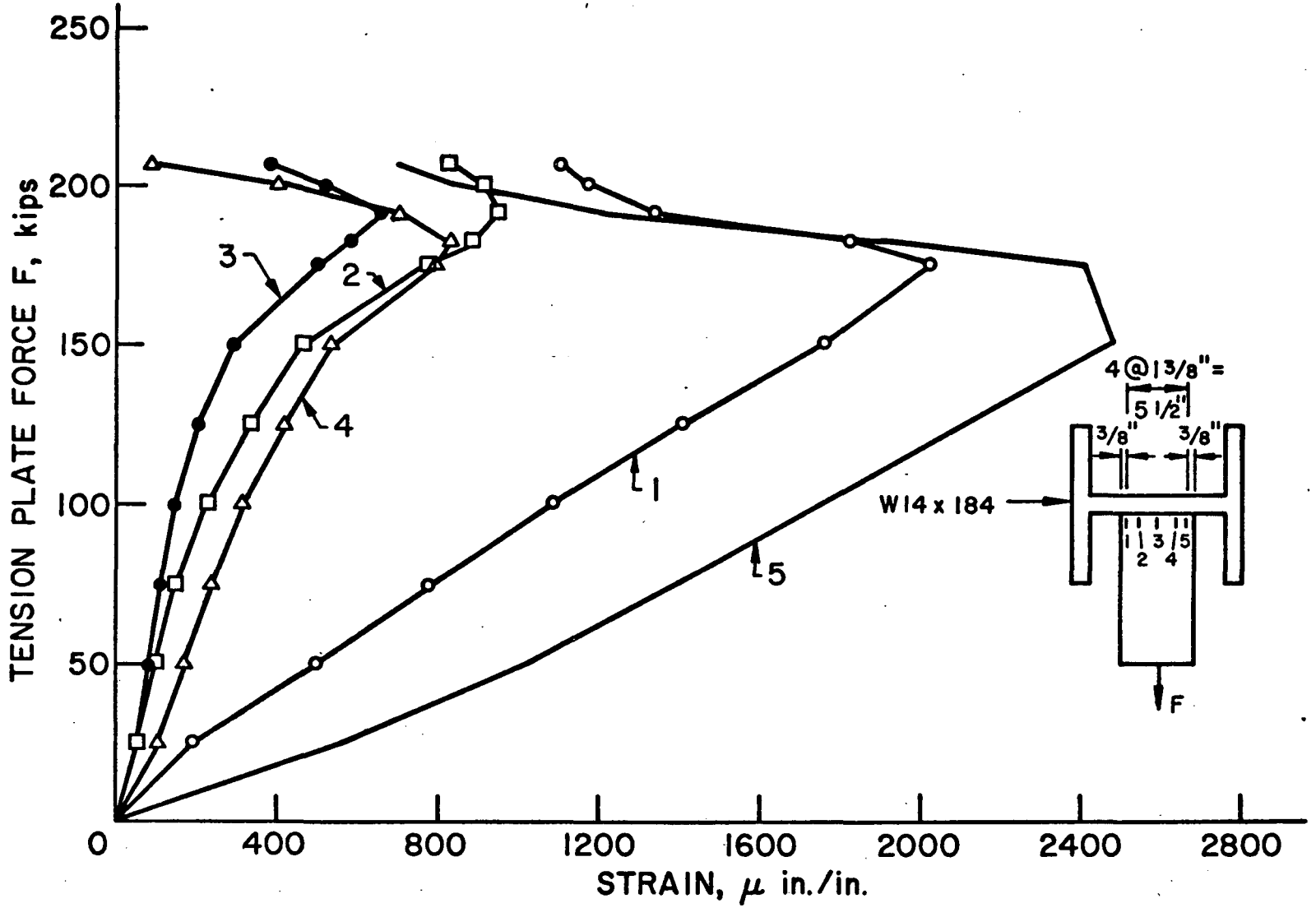

Fig. 36 Strains Measured on Tension Flange Plate of Test 14A

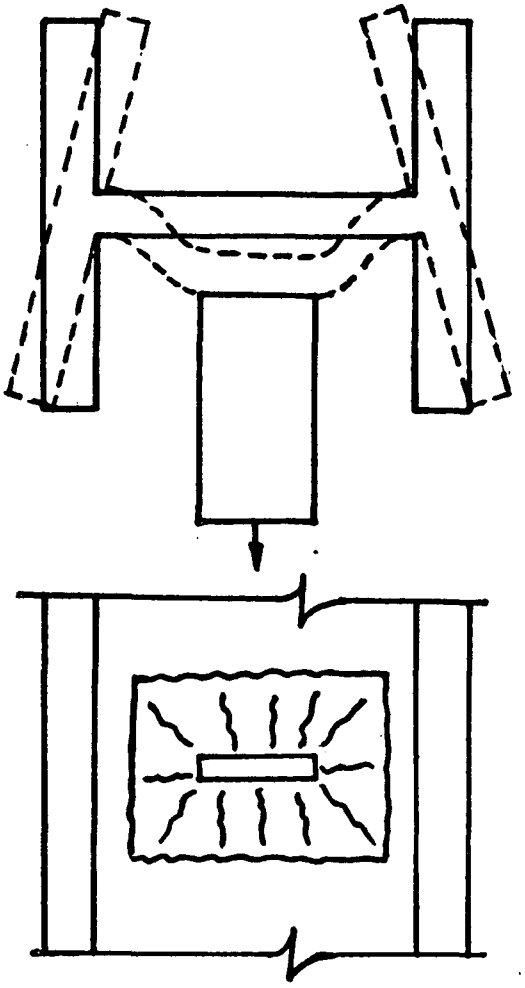

Fig. 37 Membrane Action of Column Web
for Test A

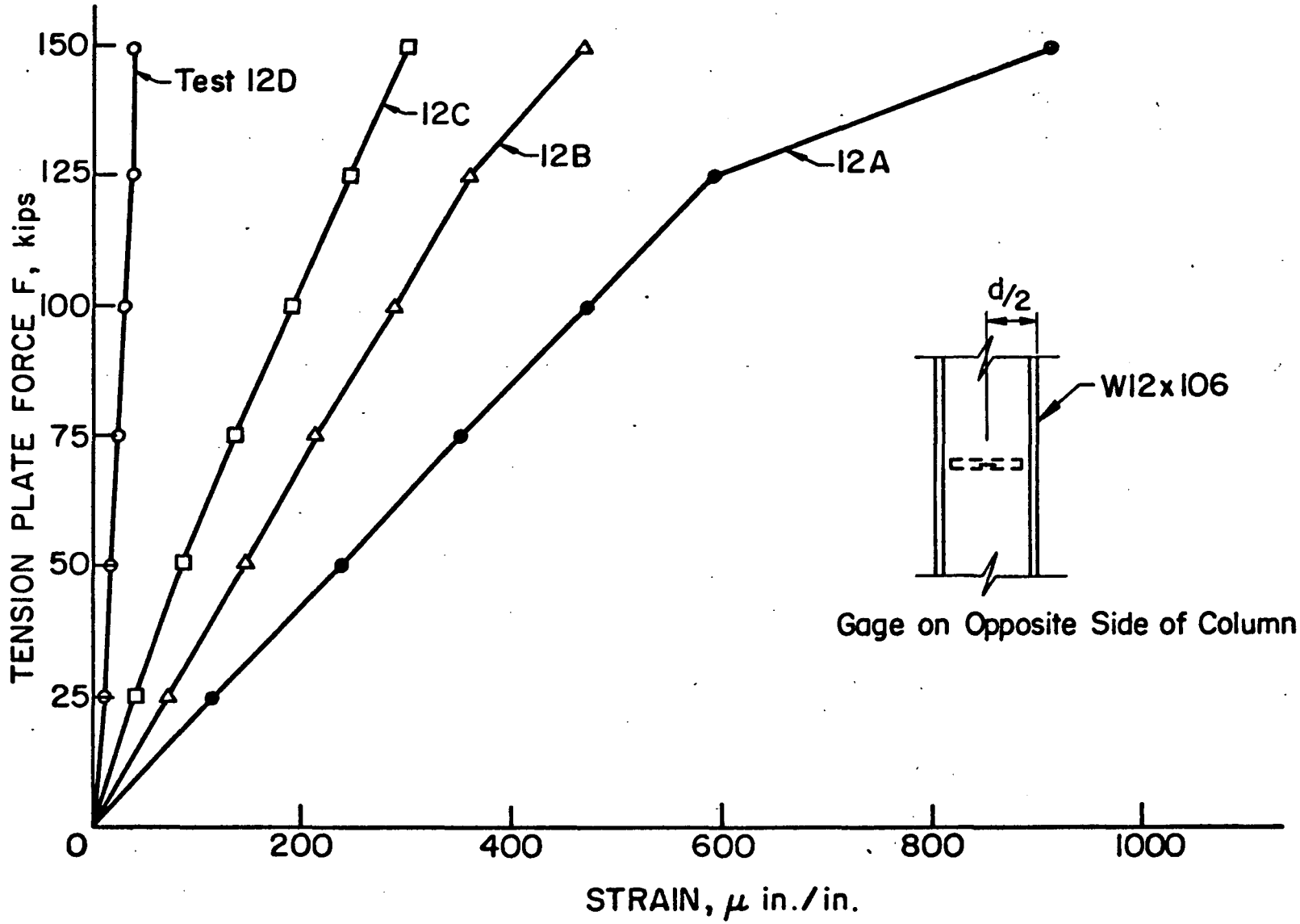

Fig. 38 Compressive Strain in Column Web

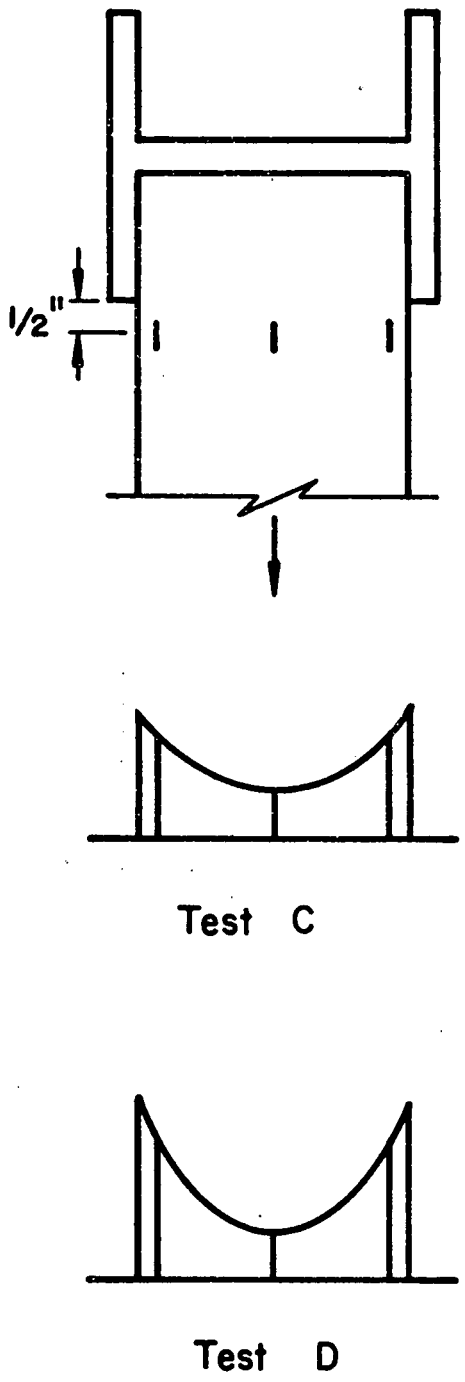

Fig. 39 Flange Plate Stress Distributions for Tests C and D